Validation and Calibration Needs of MITSIM

by

Susan (Xiujuan) Wang

M.A in Economics, Nankai University,1991

Submitted to the Department of Civil & Environmental Engineering
in partial fulfillment of the requirements for the degree of

Master of Science in Transportation

at the

Massachusetts Institute of Technology

August 1997

Author _____
Department of Civil and Environmental Engineering
August, 1997

Certified by _____
Moshe Ben-Akiva
Professor of Civil and Environmental Engineering
Massachusetts Institute of Technology
Thesis Supervisor

Certified by _____
Haris N. Koutsopoulos
Associate Professor of Civil and Environmental Engineering
Carnegie Mellon University
Thesis Supervisor

Accepted by _____
Joseph M. Sussman
Chair, Departmental Committee on Graduate Studies

Validation and Calibration Needs of MITSIM

by

Susan (Xiujuan) Wang

Submitted to the Department of Civil & Environmental Engineering
in partial fulfillment of the requirements for the degree of

Master of Science in Transportation

Abstract

MITSIM is a microscopic traffic simulator that has been developed for evaluation of dynamic traffic management system. In this thesis, we examine validation and calibration needs for MITSIM utilizing both macroscopic traffic properties and microscopic traffic characteristics.

We first review MITSIM's modeling structure and establish the connections between macroscopic traffic properties and microscopic model parameters. Second, we assess the capacity predicted by MITSIM and validate the basic flow-speed-density relationships using sensor outputs. Third, we study MITSIM's ability to replicate the traffic characteristics of a weaving section using field trajectory data from the Capital Beltway network. Finally, we compare HCM predictions of weaving and non-weaving speeds with those from MITSIM simulations, and perform a sensitivity analysis on weaving length.

We find that: (i) the capacity and flow-speed-density relationships predicted by MITSIM consistent to those found in the field; (ii) MITSIM can simulate traffic flow, weaving and non-weaving speeds reasonably well; however, its performance in simulating lane speed and density needs improvement; (iii) comparisons of the simulated headways, and mandatory lane changes to those from the field indicate that the need for more calibration of model parameters.

Thesis Supervisor: Professor Moshe E. Ben-Akiva
Civil and Environmental Engineering
Massachusetts Institute of Technology

Thesis Supervisor: Professor Haris N. Koutsopoulos
Civil and Environmental Engineering
Carnegie Mellon University

Acknowledgments

I would like to take this opportunity to thank my advisors, Professor Moshe Ben-Akiva and Professor Haris Koutsopoulos, for their invaluable advice and guidance throughout my Masters study at MIT. Without their support, this thesis would not have been possible. Professor Koutsopoulos has spent a lot of time working with me. His mastery of the traffic theories and modeling systems has provided me with many constructive suggestions.

My gratitude also go to Mr. Anthony Hotz, who has been my supervisor in the early stage of my thesis. I will forever cherish his encouragement, support, friendship and help during the difficult times in my research.

I would like to thank Rabi Mishalani, and Mithilesh Jha, for their advice in the early stage of my research. Their technical expertise and help were always available when needed.

Thanks also go to:

- Qi Yang for his technical help in using the simulator.
- Professors Cynthia Barnhart, Ismail Chabini, Ralph Gakenheimer, and Nigel Wilson ; and staff including Julie, Lisa, Cheryl, and many others, for their friendship and help.
- Ms. Cythia Stewart for her understanding, encouragement, and help.
- Friends at the Intelligent Transportation Systems Program including Alan, Costas, Dave, Jon, Kazi, Michel, Masroor, Nadine, Owen, Peter, Scott, Sridevi, Stanley, Winston for their understanding, cooperation, and friendship.

The financial support of MIT, Draper Laboratory, Bechtel/Parsons Brinckerhoff, and the Massachusetts Highway Department are deeply appreciated.

Finally I wish to express my deepest thanks to my husband, Tao-Shun Chou. Without his love, understanding, help and support, I can never finish this thesis.

Contents

Chapter 1

Introduction

Traffic simulation is often used to perform evaluations related to freeway planning, designs and operations. Since these decisions can involve millions of dollars, the accuracy and the appropriateness of a selected model are of considerable importance. The accuracy of a simulation model can be quantified by a validation process.

Simulation validation is the procedure for determining whether there is a sufficient agreement between a particular model and the actual system being modeled. A MIcroscopic Traffic SIMulator (MITSIM[1]) has been developed to evaluate a number of system designs and dynamic traffic management strategies. MITSIM is currently used to evaluate control strategies for the Boston Central Artery and Tunnels (CA/T) Project. This simulator is based on various traffic models, of which car-following and lane-changing models are the key elements. Subramanian[2], Ahmed, et al. [3][4] and Yang[5] have conducted validation tests at various stages of MITSIM's development. Their efforts have focused primarily on the calibration of each component model's parameters. To date, systematic validations of these models are far from complete. There

is a need for more tests and validations in order to improve our confidence in the model.

Calibration and validation of a simulation model can occur at various levels of detail. This research focuses on the macroscopic characteristics of traffic dynamics through aggregated measures such as speed, flow, and density. In order to determine whether a model can replicate the real world traffic, the model's ability to replicate the basic relationships between the three variables must be verified. If simulated outputs cannot match the empirical data with a certain level of confidence at the aggregated level, the performance at the disaggregated level becomes even more questionable.

1.1 Literature Review

1.1.1 Traffic Simulation Models

In recent years, traffic simulation models have been extensively developed and used for evaluations of traffic control, and route guidance strategies[8]. Based on the scope and details of the simulation, these models generally fall into three categories: microscopic, macroscopic and mesoscopic.

Microscopic models attempt to simulate the trajectories of individual vehicles. The attributes of simulated vehicles are randomly generated from certain assumed distributions. Consequently, microscopic models are stochastic given the same inputs. One simulation result is not necessarily the same with others. Microscopic models can provide an impressive amount of information, but due to the difficulty with data collection on individual vehicles, they are not as well studied as the macroscopic ones. MITSIM[1], INTRAS[9], FRESIM[10], NETSIM[11], CORSIM[12], THOREAU[13], FLEXSYT-II[14],

and AIMSUM2[15] are examples of traffic simulators in this category.

Macroscopic models simulate the behavior of the traffic stream as a whole. Traffic flows are approximated as fluids. Vehicle movements in the network are modeled in accordance with the assumed speed-density relationships. Macroscopic models are deterministic, that is, repeated realizations (i.e. simulations) of the same operating conditions generate non-varying predictions. Macroscopic models are well studied and documented, but for many applications, they do not supply enough information at the required level of detail. FREFLO[16], NETVAC[17], AUTOS[18], METANET[19], and METACOR[20] are some of the models belonging to this category.

Mesoscopic simulation models are hybrids of macroscopic and microscopic models in terms of simulation logic and representation of traffic flows. Like microscopic simulation models, traffic flows in mesoscopic models are modeled in terms of individual vehicles. However, vehicle movements in the network are modeled in accordance to speed-density relationships. METROPOLIS[21], INTEGRATION[22][23], MesoTS[5] are a few models in this group.

1.1.2 Validation of Microscopic Models

Validation is an important step necessary for improving the performance of traffic simulation models. Numerous validation efforts have been undertaken in attempts to improve microscopic traffic simulation models. To put this research in perspective, we review previous validation work on microscopic traffic simulators, which are similar to MITSIM.

Validation of CARSIM

CARSIM was one of the early car-following simulation models developed in the 1980's. It can be used for simulation of freeway and street traffic under normal and stop-and-go condition, and for simulation of traffic ranging from free flow to jam density. Benekohal[25] conducted a validation at both microscopic and macroscopic levels, using three 15-vehicle platoon data, which represented regular disturbance, emergency stop, and stop-and-go operations respectively.

The model was validated by the following procedure. First, model parameters such as maximum acceleration rate, compliance level, start-up delay, reaction time, buffer space, and traffic mix, were calibrated with the field data. Second, these parameters were incorporated into microscopic and macroscopic validation tests. Third, for each type of disturbance, five simulation runs were averaged to get the microscopic and macroscopic measurements. At the microscopic level, the effect of three types of disturbance on individual vehicle trajectory, speed, and acceleration/deceleration, were investigated under high and low traffic volumes. Then individual vehicle speeds and trajectories were used as measure of performance, and compared with those from the three field platoons. At the macroscopic level, the effects of a regular and an emergency stop on average speed, flow density, and average headway were examined using high and low traffic flows. The averaged flow, speed, density and flow-speed-density relationships were used to evaluate the model's overall performance, and they were compared with those from the field.

In Benekohal's work, systematic and extensive validations were conducted at different levels. However, since the research was based on a sample population of only three 15-car platoons, the validation results may not be representative. In addition, the traffic flow was simply calculated as a product of speed and density, which could be incorrect for an unsteady traffic flow. Link capacity was treated as a given and no empirical verification of its value was done.

Validation of INTRAS

INTRAS[9], a predecessor of FRESIM[10] and CORSIM[12], is a relatively sophisticated and widely used microscopic freeway traffic simulator developed by FHWA. It was designed for freeway traffic simulations and structured to facilitate the evaluation of different incident detection algorithms and ramp metering strategies. Extensive validation and calibration work has been done to enhance the model performance. Among them, the work done by R.L. Cheu et al.[24] and Cassidy et al. [7] are representative.

Cheu's research represented an initial validation effort, which focused on the calibration of specific model parameters, in particular the parameters in car-following and incident detection models. The study aimed at accommodating the model outputs to new traffic patterns by replacing the old parameters estimated from 70's data. with newly estimated ones from more recent data. Key parameters calibrated in the study included car-following sensitivity constants, minimum car-following distance, vehicle length, effective detector lengths, and the INTRAS "rubber-necking" factor. Three 30-second detector station data sets on average volume and occupancy were used in the study.

These data were collected from loop detectors located on a 4.8-mile stretch of major freeway on the westbound SR-91 Riverside in Orange County, California. Incident-free data from 1987 were used to calibrate parameters related to the car-following model. Incident data, collected in 1990, with partial lane blockage and incident data from 1991 with entire freeway blockage were used to calibrate incident-related parameters.

The validation process consisted of two phases. First, parameters related to car-following and loop detector operations were calibrated against incident-free data. These parameters were calibrated sequentially (i.e. at any time with only the value of one of the parameters varied). As the optimum value of any particular parameter was calibrated, the remaining parameters were treated as constants. These parameters were adjusted to bring the volume and occupancy predicted by INTRAS closer to the field data, with emphasis on volume count. Once the appropriate combination of the non-incident parameters was determined, incident-related parameters were calibrated. In the second phase, the "rubber-necking" factor was calibrated using incident data. Average volume and occupancy were used as the basis for evaluating the results of the parameter calibrations. Optimal parameters were identified as the ones that produced the best matching volume and occupancy. Correlation coefficients between field and simulated flow, occupancy, and slopes of fitted straight lines that pass through the origin derived from simulated and field data plots were used as performance measures.

The validation results indicated that the chosen car-following parameters were the best among the attempted values in describing driver behavior With these car-following

parameters, INTRAS was capable of "moving" vehicles at volumes very close to the actual counts made on the freeway. However, the loop detector occupancies were always lower than the values obtained from the field. The "rubber-necking" study showed that it was not necessary to assign any rubber-necking factor in the incident specification. Putting the actual incident blockage into the simulation was sufficient to produce an occupancy pattern closely resembling the actual traffic operations during incidents.

Validation of Enhanced INTRAS

Compared with the work of Cheu et al., the validation study by Cassidy et al.[7](1995) for the enhanced version of INTRAS, is more comprehensive. The focus is not just on parameter adjustment. Instead, the model's overall performance in replicating real world traffic operations, the model's sensitivity to network geometric changes, and the compatibility between model algorithms and actual traffic dynamics, were emphasized. In this research, INTRAS was validated and evaluated along with other widely used commercial traffic simulators, such as FREQ, FREFLO. These models were evaluated and validated by the same two 60-second sensor data sets. One of the data sets was collected from a 10-mile freeway segment selected in the westbound of Route 50, just east of downtown Sacramento CA, where recurring congestion was consistently observed. The other one was gathered from a simple 1-mile "straight-pipe" freeway section, chosen from the northbound of the I-880, where a regular queuing from downstream incidents and/or spill-overs from off-ramps was observed.

As the only microscopic simulator in the study, INTRAS was validated and eval-

uated using the following procedure:

- First, field traffic patterns were extracted from station-averaged field data, so that they could be used as "target" performance measurements in the following calibration and validation process;

- Second, one hour Route-50 data was used for calibrating basic parameters such as vehicle free-flow speed for each link, and vehicle mix. Information on locations of upstream warning message signs, locations of detectors, lane utilization rates, the physical lengths of acceleration and deceleration lanes was also collected. Meanwhile, sensitivity analysis was also conducted to test the impact of the locations of sensors and message sign on simulated traffic.

- The calibrated parameters were incorporated into the simulations of Route-50 and I-880. Empirical detector data of flows, average speeds, along with travel times measured by tachograph vehicles, were used as main performance measures, and compared with INTRAS generated values.

Results from the validation of INTRAS indicate that:

- INTRAS cannot simulate a network of extended length. The simulation of the 10-mile Route-50 network was consistently terminated prematurely by the over-jammed traffic predicted by the simulator. Although a lower queue discharge rate was attributed as one of the causes, the analysis also showed that the over-estimation of traffic congestion around a bottleneck can be reduced by dividing

the network into smaller segments.

- The alteration of the lengths of acceleration and deceleration lanes can significantly affect the simulation outputs. This indicates that the merging and diverging logic cannot replicate the actual operation characteristics precisely.

- The sensitivity tests of sensor location indicated that close agreement between observed and simulated speeds could only be achieved by moving simulated detectors away from on-ramp junctions. This suggest that the car-following logic was over-sensitive to the impact of merging vehicles.

- The validation with the I-880 data showed that the microscopic logic may have problems in replicating high demand traffic. Although the simulated capacity seemed well below that of the field, the researchers did not analyze the cause of the problem.

Besides the problems with the INTRAS model itself, there are problems with the validation process. First, geometry information, such as the lengths of acceleration/deceleration lane, link capacity, positions of sensors and message signs, should all be given as inputs. Estimation of these basic inputs by selecting trials that give the best match cast doubts on the objectiveness of the model. Second, all the validation efforts were based on field sensor data. As a result, the correctness of the validation results depends on the accuracy of the data. However, there are many difficulties with sensor data:

- Theoretically, OD flows can be estimated from the sensors on the mainline freeway, but due to lack of sensor on the ramps, or the failure of these sensors, the accuracy of the OD flows used in the simulation becomes questionable.

- Vehicle mix cannot be directly inferred from the field detector counts.

Validation of MITSIM

As we mentioned before, MITSIM has been validated during various stages of the development. The validation work has attempted to improve specific model performance by adopting newly estimated parameter values based on field data. These efforts can be summarized as follows:

- Calibration and validation of the lane-changing model - In the development of lane-changing model, Ahmed[4] used FHWA data set on vehicle trajectories[26] to estimate and validate lane-changing parameters. In his validation process, statistical properties of these parameters were calculated and compared with values found in literature, and the best fit parameters were then incorporated into MITSIM. The simulation results were compared with field data using measurements of speed and flow.

- Calibration and validation of the car-following model - Subramanian[2] estimated the car-following model parameters using the FHWA data set[26] Performance of the new parameters were then compared with previous guesstimates of the parameter by using flow and speed data at various sensor stations. The newly

calibrated car-following model improved the fit to the field data.

- Overall validation of MITSIM - Yang and Koutsopoulos[1][5] evaluated the overall performance of MITSIM using a 5.9-mile stretch of I-880 north freeway network. Simulated flow, speed, occupancy were compared with field observations. Their work showed that MITSIM tends to underestimate occupancy in certain areas.

Although many specific models were improved by these validations, their overall effectiveness in MITSIM, particularly at critical areas such as weaving and ramp areas remain to be tested. The impact of ramps on lane-changing behaviors, and hence the overall speeds deserve further exploration. Finally, the theoretical assumptions that underlie the models, such as lane-changing and headway distributions, have not been empirically verified.

1.2 Thesis Objectives

In this thesis, we set out to achieve the following objectives in the validation of MITSIM:

- assess the capacity predicted by MITSIM (Ch 3).
- validate basic macroscopic traffic relationships using sensor outputs from MITSIM (Ch 3).
- study the ability of MITSIM to replicate the traffic characteristics of a weaving section using field trajectory data (Ch 4).

- compare HCM predictions of weaving and non-weaving speeds with those from MITSIM simulations (Ch 5).

- conduct a sensitivity analysis of weaving length and compare the precision of MITSIM predictions with those of HCM (Ch 5).

From the literature review section, it is clear that previous work primarily focused on freeway main sections. Weaving sections, which influence the performance of the freeway system significantly, and simulations are needed the most, have not been systematically studied. Moreover, most of existing work used either sensor or platoon data in validating the models, which can have serious limitations. In this thesis, we will use real world, vehicle trajectory data collected by FHWA photographic film and manually processed. The site chosen for our field study is a ramp weaving area on I-95 in the Prince Georges County of Maryland.

1.3 Thesis Outline

The remainder of the thesis is structured as follows:

Chapter 2 reviews the MITSIM model structure, macroscopic traffic properties of interest, and the interrelationships between macroscopic and microscopic model parameters. Chapter 3 presents a simple case study on MITSIM's maximum lane vehicle loading capacity, and validates the basic relationships among traffic flow, speed and density. Chapter 4 describes weaving traffic characteristics of the Capital Beltway data, and presents the main validation results of MITSIM on a weaving section by comparing its

outputs with those from the field. Chapter 5 evaluates MITSIM's overall performance on a weaving section by examining its sensitivity to weaving length changes, and comparing its predictions with those from HCM. Chapter 6 concludes this thesis by highlighting the main contributions and suggesting directions for future research.

Chapter 2

MITSIM Model and Macroscopic Properties

MITSIM, the MIcroscopic Traffic SIMulator, is designed to take traffic control and routing information as inputs, and produce vehicle trajectory outputs for evaluating traffic management systems. Its capabilities include: (i) generating real-time simulation data on vehicles' spatial and temporal trajectories in the network, (ii) providing real-time sensor data that mimics the surveillance capacities of the traffic management systems in an ITS environment, (iii) calculating a set of measures of effectiveness (MOE) that describes the performance of the system under evaluation.

In order to validate MITSIM, we first need to understand its model structure and the key parameters that control the models. It is also important to know the interrelationships between macroscopic traffic properties and microscopic model parameters. The purpose of this chapter is to make these preparations for the validation of MITSIM. The outline of the chapter is as follows: In *Section* 2.1, we briefly review the MITSIM model structure and describe key parameters that control the models. In *Section* 2.2,

we describe the main macroscopic traffic properties that of our validation interest. In *Section* 2.3, we present the mathematical relationships between macroscopic traffic properties and microscopic model parameters. A summary of this chapter is presented in *Section* 2.4.

2.1 MITSIM Modeling Structure

As a microscopic traffic simulator, MITSIM attempts to analyze individual vehicle trajectories by simulating each driver vehicle unit in the changing environment of traffic flow, roadway configuration, and traffic signs/signals. In the simulation, a vehicle is represented by a set of deterministic and type specific parameters, such as *normal deceleration rate*, *maximum acceleration rate*, and *maximum speed*. The driver behavior is represented by randomly assigned parameters which follow pre-specified distributions when the vehicle enters the network. Driver behavior parameters include the *desired speed* of the driver, his/her *compliance* to each type of traffic signs and signals, and his/her overall *aggressiveness*.

The flowchart of MITSIM is shown in Figure 2.1. The simulation procedure can be roughly divided into three phases: initialization, update, and advance phase. In the initialization stage, MITSIM loads in simulation parameters, traffic signs/signals, incident information, OD trip tables, and creates the appropriate simulation environment. In the update phase, MITSIM controls the vehicle movements, including the interactions of vehicles with one another, responses to traffic controls, and changes of vehicles' pre-

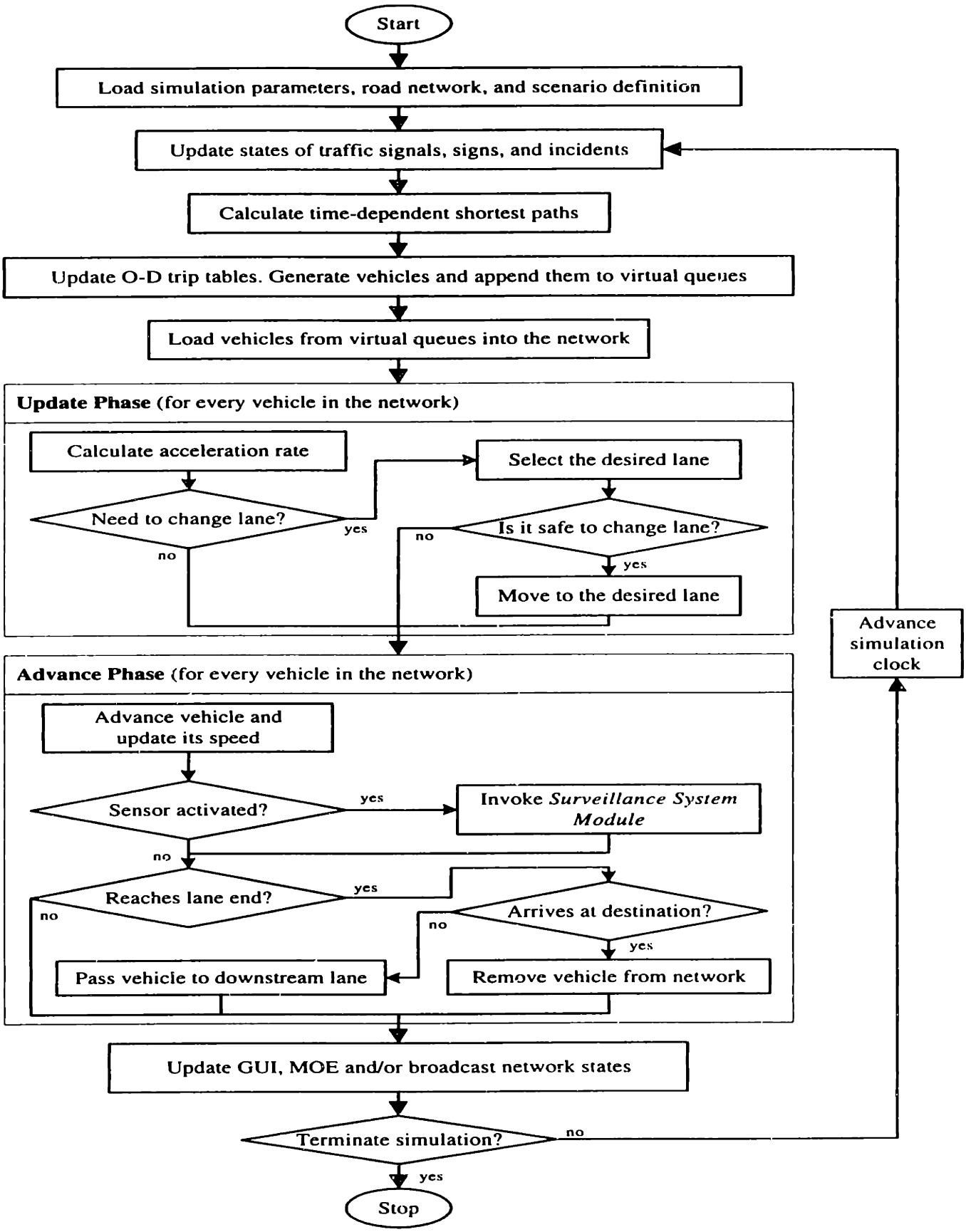

Figure 2.1: MITSIM modeling structure overview (Source:Yang[5])

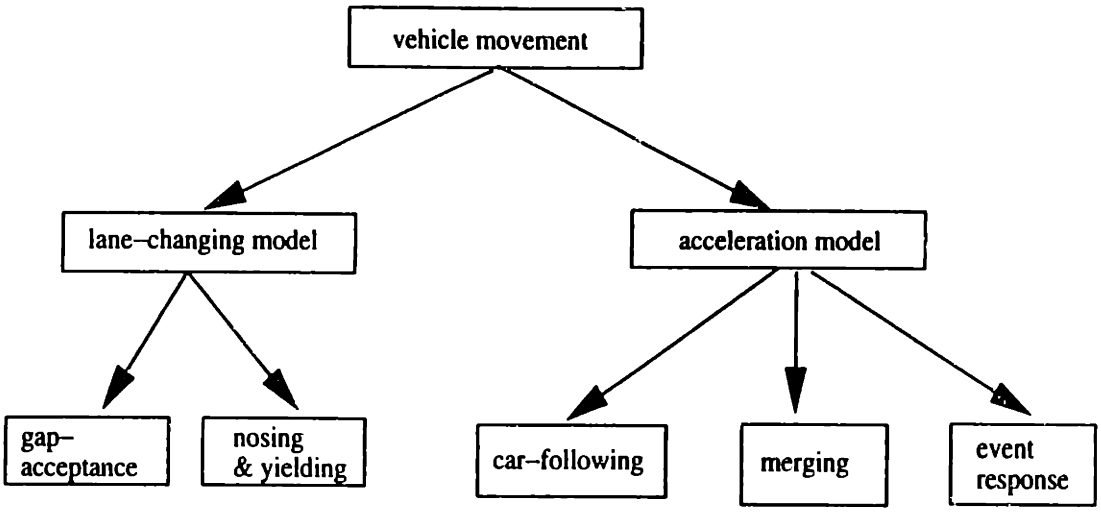

Figure 2.2: MITSIM vehicle movement modeling structure.

ferred lanes. In the advance phase, MITSIM checks all the updated vehicles and driver states, making sure that the motion of each vehicle is consistent with the parameters and states calculated in the update phase.

The movement of every vehicle in MITSIM is controlled by both the *acceleration model* and the *lane-changing model*. The acceleration model is composed of car-following, merging, and event response models. The car-following model computes the acceleration or deceleration rate of a vehicle in terms of its relationship with the leading vehicles. The merging model guides the vehicle as it moves into a merge area. The event response model captures drivers' response to events like traffic signs and signals, incidents, and toll booth. The relationship of these models is shown in Figure 2.2. The lane changing model controls the details of lane switching. It involves the modeling of gap acceptance, nosing, and yielding.

2.1.1 Acceleration Models

Acceleration models are engaged in a vehicle whenever it needs to: (i) achieve a desired speed, (ii) react to the vehicles ahead (car-following), (iii) perform a lane changing or merging maneuver, and (iv) respond to events (e.g. red signals and incidents). The acceleration/deceleration rate to be implemented is determined by the most constraining condition encountered at the time.

Car-following Model

Car-following model forms the basis of all models in the category of acceleration models, in which merge and event-response models can be regarded as extensions of the car-following model with additional constraints. The car-following model calculates a vehicle's acceleration rate based on its relationship to the leading vehicles. It is developed on the basis of Herman's model. Depending on the relative magnitude of the current headway to the pre-determined headway thresholds h^{upper} and h^{lower}, a vehicle is classified into one of the three regimes: *free-flowing*, *car following*, and *emergency decelerating*. The three regimes are shown in Figure 2.3.

If a vehicle has a headway between the upper bound h^{upper} and the lower-bound h^{lower}, it is in the car-following regime. The acceleration rate is computed using Herman's general car-following model[38]:

$$a_n = \alpha^{\pm} \frac{v_n^{\beta^{\pm}}}{(x_n - x_{n-1})^{\gamma^{\pm}}} (v_{n-1} - v_n) \tag{2.1}$$

where x_{n-1} and v_{n-1} are the position and speed of the leading vehicle, x_n and v_n are the

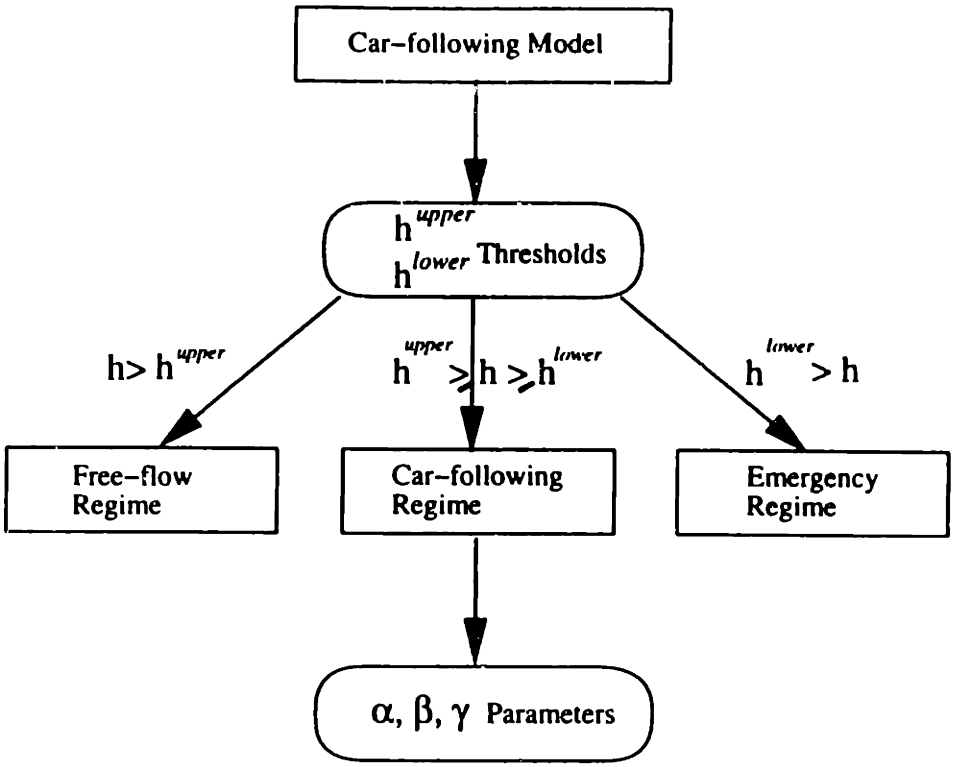

Figure 2.3: MITSIM car-following model structure

position and speed of the current vehicle, respectively. The model parameters α^+, β^+, γ^+ are used in acceleration, while α^-, β^-, γ^- are used in deceleration.

If a vehicle has a time headway larger than the pre-specified threshold h^{upper}, the vehicle is in the free flowing regime where it does not interact with the leading vehicle. In this case, if the speed of current vehicle is lower than its target speed, it accelerates at the *maximum acceleration rate* in order to achieve its target speed as quickly as possible. If the current speed is higher than the target speed, then the vehicle decelerates with the *normal deceleration rate* to slow down. If a vehicle has a headway smaller than the pre-determined lower-bound h^{lower}, it is in the emergency regime. In this case, the vehicle uses an appropriate deceleration rate to avoid collision and to extend its headway

towards a safe range.

Merging & Event Responding Models

The merging model is activated when the vehicle moves into a merge area, i.e. a geometric configuration where two or more upstream lanes are connected to a single downstream lane. It is a modified car-following model that takes additional constraints, such as right of way and merging type, into the calculation of acceleration.

Similar to merging model, event response model can also be viewed as a car-following model with special constraints. The constraints include: (i) traffic signs and signals, (ii) incidents, (iii) making a connection to the next link at the downstream node, and (iv) yielding to another vehicle switching into the same lane.

2.1.2 Lane Changing Model

In MITSIM, the other key model for the control of vehicle movement is the lane changing model. The algorithm for lane change involves: (i) checking to see if a change is necessary and define the type of the change, (ii) selecting the desired lane, and, (iii) executing the desired lane change if the gap distances are acceptable. Its modeling structure is shown in Figure 2.4.

MITSIM models the lane changing behavior of a driver starting when the driver begins to make lane-changing decision. This decision depends on the traffic conditions, driver's destination, and driver's behavior characteristics (e.g. from conservative to aggressive). MITSIM classifies lane changes into two types: *discretionary* and *mandatory*.

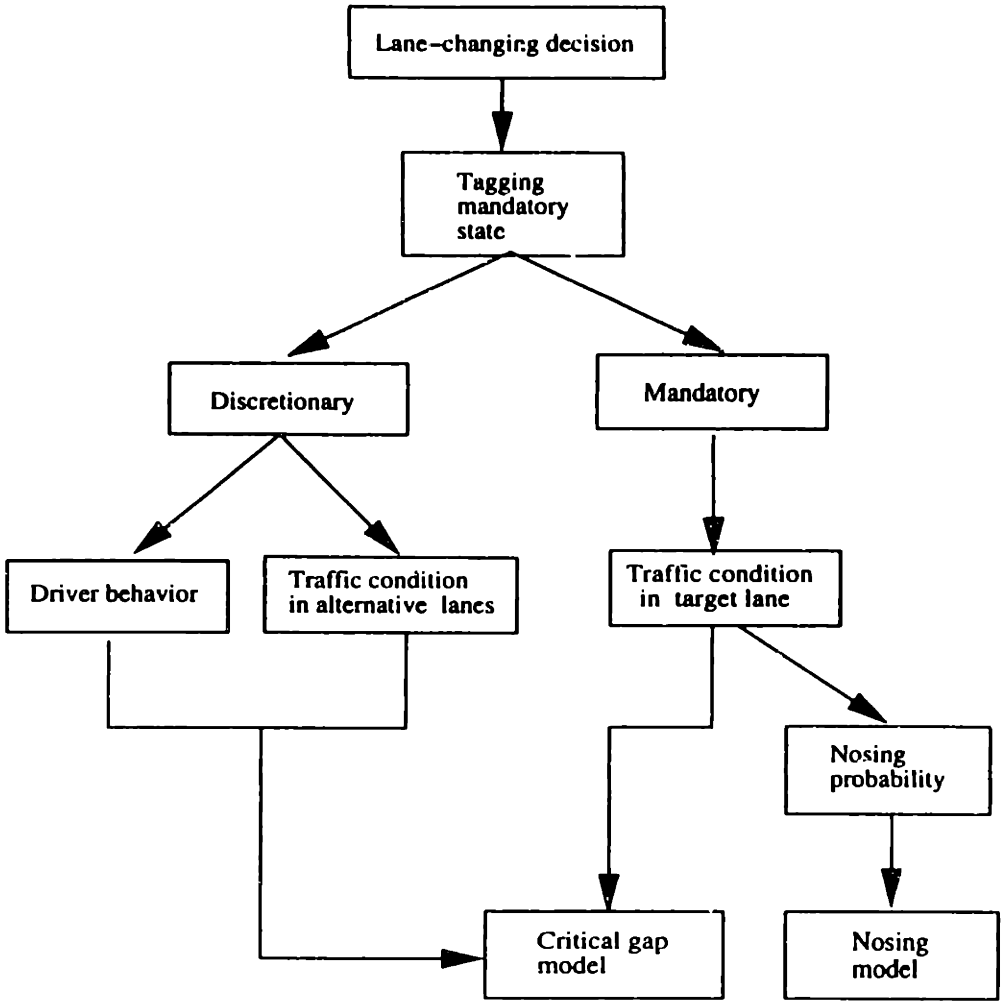

Figure 2.4: MITSIM lane-changing model structure

Discretionary lane changes occur when drivers want to attain a higher speed in an alternative lane, bypass a slower or heavy vehicle, or avoid the lane connected to a ramp. Mandatory lane changes occur when drivers change lanes in order to connect to the next link on their path, bypass a lane blockage downstream, avoid entering a restricted lane, or respond to lane usage sign and warning of lane termination.

When a driver begins to consider such lane-changes, he/she also needs to consider *when* and *where* to execute the lane change. Drivers make different decisions even if the

traffic condition they face are the same. To capture this stochastic behavior, a *mandatory state* is introduced in MITSIM for representing the probability of a lane change as the vehicle approaches various locations. The underlying probability models are functions of the distance to the downstream node, distance from a critical location (such as exit warning, message sign, etc), the number of lanes that a vehicle needs to cross in order to reach the target lane, and the general traffic condition.

A vehicle's probability of being in the mandatory state is conditioned on its state in the previous time interval. Once a vehicle has been tagged to be in the mandatory state, it remains in that state until the desired lane change has been executed, or the downstream link has been reached.

2.2 Macroscopic Traffic Properties

In our validation of MITSIM, we are interested in the operational states predicted by MITSIM for any given uninterrupted freeway facility. Each operational state can be fully described by three primary measures, *speed, volume*, and *density*.

Speed

Speed (or its reciprocal – travel time) is a fundamental measure on the quality of traffic service provided to the drivers. One commonly used speed measure, the *space mean speed*, is defined as the length of the segment divided by the average running time of vehicles traversing the segment. Another speed measure, the *time mean speed*, is defined as the arithmetic average of the speeds of vehicles that pass a given point on the

highway. Two speed parameters, the *free-flow speed* and the *optimum speed* are often used to characterize freeway facilities. They represent, respectively, the the maximum speed that the freeway facility can provide, and the optimal level of service a system can afford when traffic flow reaches capacity.

Flow

Traffic flow or volume is another key macroscopic traffic characteristic representing the traffic load to the transportation system and the interactions among the "loadings". It is defined as "the total number of vehicles that pass over a given point or section of a lane or roadway during a given time interval". It is expressed in an hourly rate on a per lane basis (veh/hr/lane) [6]. *Maximum flow* or *capacity* is a unique flow parameter that characterizes the highest operational performance of a freeway system.

Density

Density is defined as "the number of vehicles occupying a given length of a lane or roadway at a particular instant" [6]. It is an important measure for uninterrupted flow facilities because it describes the proximity of vehicles to one another. It also reflects the freedom to maneuver within the traffic stream, and characterizes the quality of traffic operations from viewpoints of the drivers and system operators. Two basic density parameters of a freeway facility are the *jam density* and the *optimum density*. Jam density describes the traffic under congested condition, when both flow and speed approaches zero. Optimum density represents the traffic condition when flow reaches capacity.

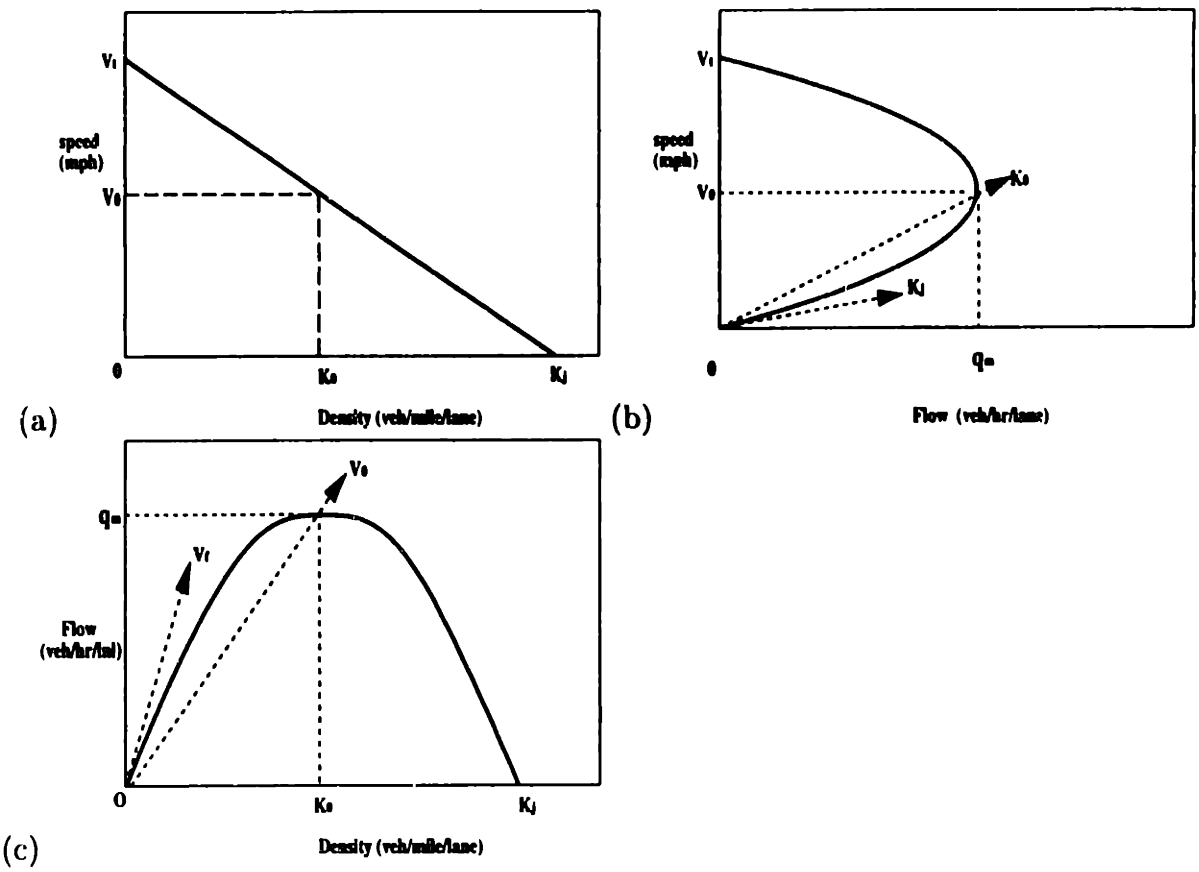

Figure 2.5: Simplified relationships between speed, flow, and density on an uninterrupted flow facility.

Relationships between Speed, Flow, and Density

There are many macroscopic theories describing the relationships between speed, flow, and density. A theoretically simplified plot is shown in Figure 2.5. In this graph, a linear speed-density relationship is assumed. Speed, flow and density follows the equation: flow = speed × density. The key parameters, such as maximum flow (q_m), free-flow speed (v_f), optimum speed (v_0), optimum density (k_0), and jam density (k_j), determine the operation of an uninterrupted traffic stream, and form the basis of capacity analysis.

The three diagrams shown in Figure 2.5 are redundant. It is obvious that if

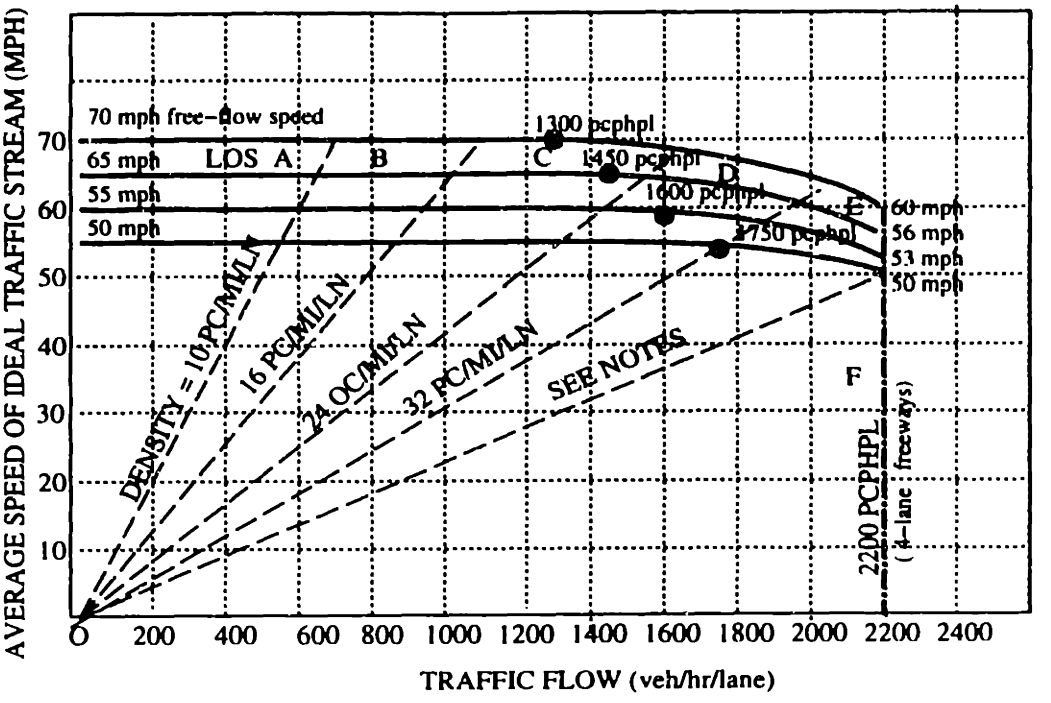

Figure 2.6: Field observations of flow-speed relationship under ideal traffic condition. (Source: Highway Capacity Manual, special report 209, third edition)

any one relationship is known, the other two are uniquely defined. The speed-density relationship is used in most theoretical work, because for every density value, there is a unique value of speed, and vice versa, which is not true in the other two relationships. However, density is very difficult to measure directly in the field. As a result, speed-flow relationship is often used in practice, assuming that key parameters are defined clearly and that the traffic regime is known. Field observations of speed-flow relationship under ideal traffic condition are shown in Figure 2.6.

Level of Service

Based on the values of speed, density, and flow, *level of service* can be assigned to describe the operational condition. The assignment of level of service can be demonstrated through the example shown in Figure 2.6. From the figure, we see that speed is nearly constant over a wide range when flow is lower than 1,200 veh/hr/lane. Therefore, speed is not an adequate measure of performance for level of service determination. Density, the measurement of freedom to maneuver within the traffic stream and proximity to other vehicles, is often a better measure for defining the level of service.

2.3 The Interrelationships Between Macroscopic and Microscopic Models

Macroscopic and microscopic are the two main approaches to studying traffic flow characteristics of highways. The microscopic approach sometimes is referred to as the car-following theory, take as its elements, individual vehicle speeds and headways. The macroscopic approach deals with traffic stream flows, densities, and average speeds. Many studies have shown that these two approaches are interrelated.

2.3.1 Generalized Car-following Model

The challenge to describe vehicular flow in a microscopic manner have led Pipes[41] to formulate the phenomena of the motion of pairs of vehicles following each other according to the expression of:

$$x_{n-1} - x_n = L + s(v_n) \tag{2.2}$$

In other words, each car-following vehicle maintains a separation distance of $(x_{n-1} - x_n)$, proportional to the speed of the subject vehicle (v_n), plus a distance of standstill space headway (L). The derivative of this equation, or $a_n = (v_{n-1} + v_n)/s$, is generally referred to as the basic equation of the car-following model. From this basic stimulus-response relation came a series of advance car-following models. The fifth generation model (i.e. Herman's model)[38] is the one used in MITSIM:

$$a_n(t+T) = \alpha \frac{v_{n-1}^{\beta}(t+T)}{(x_{n-1}(t) - x_n(t))^{\gamma}} \tag{2.3}$$

It is a general expression of other car-following models. It can be seen that most other models are special cases of this model by setting β and γ to some special values.

2.3.2 Macroscopic Traffic Models

The development of macroscopic traffic theories dates back to 1935, when Greenshield[43] put forward a hypothesized linear relationship between speed and density,

$$v = v_f\,(1 - k/k_j) \tag{2.4}$$

where v_f is the free-flow speed, k_j is the jam density, v is the speed, and k is the density.

Then later in 1959, Greenberg[44] proposed another macroscopic flow model by using the analogy of the traffic-flow situation with the problem of one-dimension fluid flow. From the equation of continuity and the equation of motion, the relationship between speed and density can be expressed as:

$$v = v_f\ \ln(k_j/k) \tag{2.5}$$

where k_j is the jam density.

In 1960, Underwood[45] proposed an exponential speed-density relation of

$$v = v_f \, e^{-k/k_0} \tag{2.6}$$

where k_0 is the optimum density. Underwood was disturbed by the flow speed going to infinity in the Greenberg model.

After a careful study of the speed-density relationship and previous traffic models, Edie[46] hypothesized that there were two regimes of traffic flow: free-flow and congested-flow. He proposed that the Underwood's equation be used for the free-flow regime, and the Greenburg's equation be used for the congested regime.

Using the fluid-flow analogy approach earlier by Greenburg but employing a more general derivation of this problem, Drew[47] proposed a speed-density relation of:

$$v = v_f \, [1 - (k/k_j)^{(n+1)/2}] \quad \text{for } n > -1 \tag{2.7}$$

Drake et.al.[39] reported on the application of a bell-shaped curve which gave satisfactory results when compared to speed-density measurements. Their proposed speed-density relation is

$$v = v_f \, e^{-1/2(k/k_0)^2} \tag{2.8}$$

2.3.3 The Interrelationships Between Microscopic and Mascroscpic Models

The interrelationship between macroscopic and microscopic traffic theories was first found by Gazis et.al[38]. It was shown that several proposed macroscopic traffic theories

are mathematically equivalent to the generalized microscopic expression of Herman's model, provided proper values are selected for the model parameters of β and γ. A further study by Gazis et.al.[42] has shown that by integrating Herman's car-following model, the following equation can be obtained:

$$f_\beta(v) = c' + cf_\gamma(s) \tag{2.9}$$

where

f_p is a function of $p = \beta$ *or* γ, and

$$f_p(v) = \begin{cases} v^{1-p} & \text{if } p \neq 1 \\ \ln(v) & \text{otherwise} \end{cases}$$

v = steady-state speed of a traffic stream;

s = constant average spacing; and

c, c' = coefficients related to v_f, k_j, β, and γ.

By assuming the value of c' as:

$$c' = f_\beta(v_f) = \begin{cases} f_\beta(v_f) & \text{if } \beta > 1,\ \gamma \neq 1; \text{or } \beta = 1,\ \gamma > 1 \\ cf_\gamma(s_j) & \text{otherwise, except } \beta = 1,\ \gamma < 1 \end{cases}$$

following the equations of $q = kv$ and $k = 1/s$, and using the general solution of Equation 2.9, the steady flow speed-density equations for different β and α can be derived. They are shown in Tables 2.1 and 2.2.

For example, if $\beta = 0$ and $\gamma = 1$, then the generalized car-following model is reduced to the the Gazis et.al.'s car-following model, i.e.

$$a_n(t + \Delta t) = \frac{\alpha}{x_n(t) - x_{n+1}(t)}[v_n(t) - v_{n+1}(t)] \tag{2.10}$$

Table 2.1: Steady-state flow equations for different β and γ values (Source:[30])

	$\beta < 1$	$\beta = 1$	$\beta > 1$
$\gamma < 1$	$v^{1-\beta} = ck_j^{\gamma-1} + ck^{\gamma-1}$	Boundary conditions not satisfied	$v^{1-\beta} = v_f^{1-\beta} + ck\gamma - 1$
$\gamma = 1$	$v^{1-\beta} = c\ln(\frac{1}{k_j}) + c\ln(\frac{1}{k})$	$\ln v = c\ln(\frac{1}{k_j}) + c\ln(\frac{1}{k})$	$v^{1-\beta} = c\ln(\frac{1}{k_j}) + c\ln(\frac{1}{k})$
$\gamma > 1$	$v^{1-\beta} = ck_j^{\gamma-1} + ck^{\gamma-1}$	$\ln v = \ln v_f + ck^{\gamma-1}$	$v^{1-\beta} = v_f^{1-\beta} + ck^{\gamma-1}$

If we integrate the above equation with respect to t, it yields:

$$v_{n+1} = \alpha\,[\ln(x_n - x_{n+1})] + C_1 \tag{2.11}$$

If we substitute v for v_{n+1}, and $1/k$ for $x_n(t) - x_{n+1}(t)$, then we get

$$v = \alpha\ \ln(1/k) + C_1 \qquad \text{or} \qquad v = \alpha\ \ln(C_2/k) \tag{2.12}$$

where $C_2 = e^{C_1/\alpha}$. When $k = k_j$, vehicle speeds are zero, i.e. $v = 0$, we get

$$\alpha\ \ln(C_2/k_j) = 0 \tag{2.13}$$

Solving this equation for C_2, and substituting it back to equation 2.13, we get

$$v = \alpha\ (k_j/k) \tag{2.14}$$

Since $q = kv$, i.e. $q = \alpha k \ln(k_j/k)$. When $k = k_0$, traffic flow reaches its maximum, or $dq/dk = 0$, then $\alpha \ln(k_j/k_0) = 0$, and $k_0 = e/k_j$. Substituting this solution back to Eq. 2.14, we finally get

$$v = v_f\ \ln(k_j/k) \tag{2.15}$$

which is exactly the Greenburg model we saw in the previous section. A further exploration of Table 2.1 gives the corresponding macroscopic models under different choices of β and γ. It is shown in Table 2.2.

Table 2.2: Existing traffic flow models derived from generalized model (source:[30]).

	$\beta = 1$	$\beta = 0$
$\gamma = 0$	$v = (1/k - 1/k_j)/s$	-
$\gamma = 1$	$v = v_f \ln(k_j/k)$	-
$\gamma = 1.5$	$v = v_f[1 - (k_j/k)^{1/2}]$	-
$\gamma = 2$	$v = v_f(1 - k/k_j)$	$v = v_f\, e^{-(k/k_0)}$
$\gamma = 3$	-	$v = v_f\, e^{-1/2(k/k_0)^2}$

An investigation of these two tables reveals that all of the macroscopic and microscopic models are interrelated. By using different combinations of the car-following model parameters in MITSIM, we can simulate different macroscopic traffic models.

2.4 Summary

In this chapter, we have reviewed the main model structures of MITSIM that control vehicle movement, and pointed out the key control parameters in the component models. Next, we have discussed the macroscopic traffic properties of our validation interest (speed, flow and density), along with their relationships, and related facility operational parameters. Finally, we have summarized the structures of key macroscopic traffic models, and presented the interrelationship between various macroscopic and microscopic models.

Chapter 3

Validation of Macroscopic Traffic Relationships

As discussed in Chapter 1, the simulated link capacity can significantly affect the performance of a model. Much evidence has shown that the link capacity in INTRAS was under-estimated, which accounted for many of its simulation problems. However, the researchers did not examine the simulated link capacity in the validation study of INTRAS [7]. To examine whether such a problem is present in MITSIM, and to facilitate more complicated validation studies later on, we will conduct a case study of a basic freeway section in this chapter. Our objectives are: (i) to identify MITSIM lane loading capacity, (ii) to compare simulated speed, flow, and density with those observed in the field, and (iii) to evaluate the performance of MITSIM in replicating fundamental flow-speed-density relationships.

This chapter is organized as follows: In *Section* 3.1, a simple two-lane basic freeway network is designed and tested with different demand around regular lane capacity. By searching for the minimum traffic demand that begins to generate queues, we at-

tempt to identify the maximum number of vehicles that can be loaded onto each lane in MITSIM. In *Section* 3.2, we analyze the field patterns of the flow-speed-density relationships from the Santa Monica Freeway (detector 16) data. In *Section* 3.3, using MITSIM, we vary the traffic demand and capacity, and investigate the basic speed, flow and density relationships under these varied conditions. We then compare MITSIM simulation results with those of field findings. Finally, the main results of the chapter are summarized in *Section* 3.4.

3.1 Lane Loading Capacity

To study the lane loading capacity of MITSIM, a simple 2-lane straight "pipe-line" network has been designed. It is a terrain, 3-mile long network, without any entrance and exit in the middle, and monitored by 29 sensor stations. These sensor stations are assumed to be evenly distributed, with the first one located 528 feet from the origin node. The speed limit of the network is set to be 55 mph, and the free-flow speed is 65 mph. The traffic mix is assumed to be composed of cars, with the parameters listed in Table 3.1.

Scenarios of different OD rates have been tested. In each simulation run, a constant traffic flow is loaded into the network. Each simulation is designed to run for 1.5 hours, during which the first 15 minutes are used as "warm-up" periods, the last 15 minutes are discarded, and only the remaining 60-minute data are used in the study. To identify the "critical capacity", we use the queue lengths reported from the simulation outputs

Table 3.1: Parameter of Vehicle Mix in the Lane Loading Capacity Test

Vehicle Type	Typical Length	Typical Width	Ratio	Delay at Toll Booth	ETC Prob.	Over Height Prob.	HOV Prob.
New Car	18	6	50%	1.0	0	0	0.10
Old Car	18	6	50%	1.0	0	0	0.15
Bus	40	8	0%	1.5	0	0	1.0
Trailer	50	8	0%	1.5	0	0	0
Truck	70	8	0%	2.0	0	0	0

as the main indicator. The critical capacity is the point where the traffic demand equals to lane loading capacity. When one additional vehicle is added to the demand, due to the capacity limitation, it cannot be loaded into the network, and therefore, a queue will be generated. To reduce the effect of random seeds on queue length, 10 runs of each scenario have been conducted. Each queue length used in this study is averaged over 10 runs.

Our simulation results indicate that no queue is observed when hourly OD is below $1,990$ *veh/hr/lane*. Queues begin to appear when the OD is increased to $2,000$ *veh/hr/lane*. The simulated queue length and the corresponding OD rates are shown in Figure 3.1.

From the figure, we can see that as OD flow increases, queue length increases, and the queuing time increases. Since there is no queue before the OD flow reaches $2,000$ *veh/hr/lane*, and only a small queue of about 24 vehicles is generated near the end of the simulation, we consider $2,000 \sim 2,100$ *veh/hr/lane* as the MITSIM lane loading capacity.

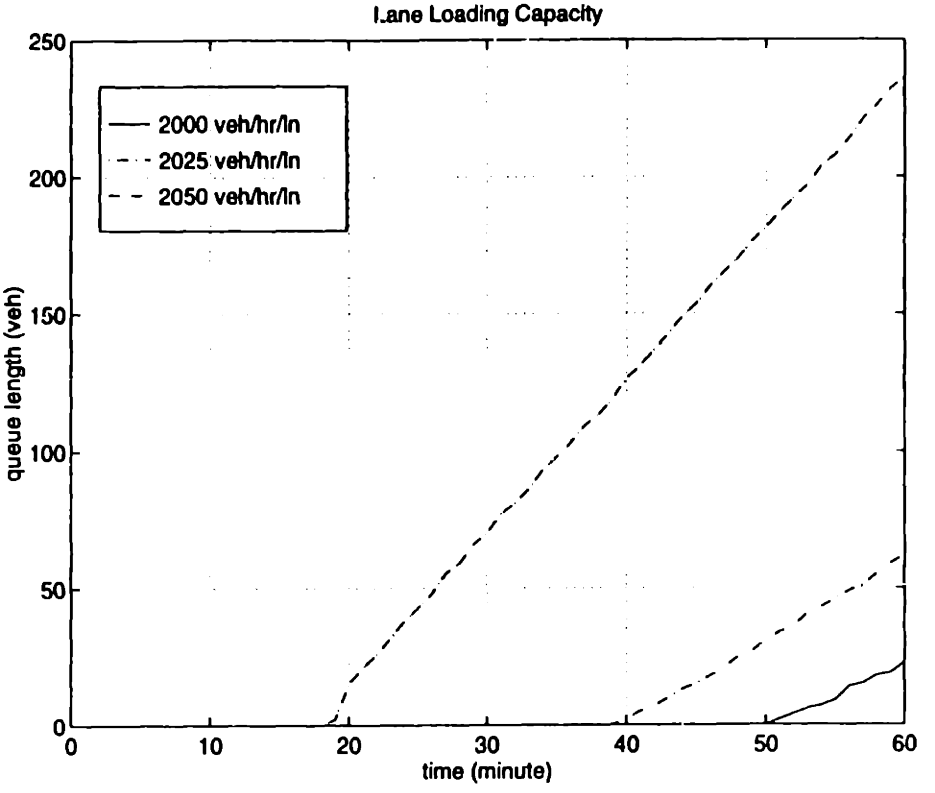

Figure 3.1: MITSIM lane loading capacity test.

3.2 Field Observations of Flow-Speed-Density Relationships

Many field analyses have been conducted by researchers in the 1960's and 1970's to study macroscopic traffic relationships. In these studies, attention was paid to the ranges of observed traffic flow, speed and density values, the consistency of data point patterns, and the parameter values estimated for macroscopic traffic models.

In this section, we chose a data set to show the field flow-speed-density patterns. The data used for this field study was obtained from the Santa Monica Freeway (detector station 16) in Los Angeles [29]. This urban roadway incorporated high design standards

and operated under nearly ideal conditions. A high percentage of the drivers were commuters who used this freeway on a regular basis. Measurements were averaged over 5-minute periods. The observed relationships between speed, flow, and density for the high-speed freeway are shown in Figure 3.2.

The field data indicate that:

- The sample displays a distribution of observed densities from near zero to 130 veh/mile/lane. No density value over 130 veh/mile/lane has been observed.

- The maximum flow or capacity appears to be just under 2,000 veh/mile/lane, and the optimum density is approximately 40 to 45 veh/mile/lane.

- The free-flow speed is slightly over 60 mph, but the jam density cannot be estimated.

- The speed-density plot exhibits a very clear data pattern and displays a slightly S-shaped curve.

- The flow-density plot also shows a very clear data pattern. The free-flow portion appears somewhat as a parabola, while the congested-flow portion is relatively flat with a tail to the right.

- The flow-speed plot displays a data pattern, but the pattern is neither completely connected nor clear. The optimum speed is not clearly defined, and can lie anyway between 35 and 45 mph.

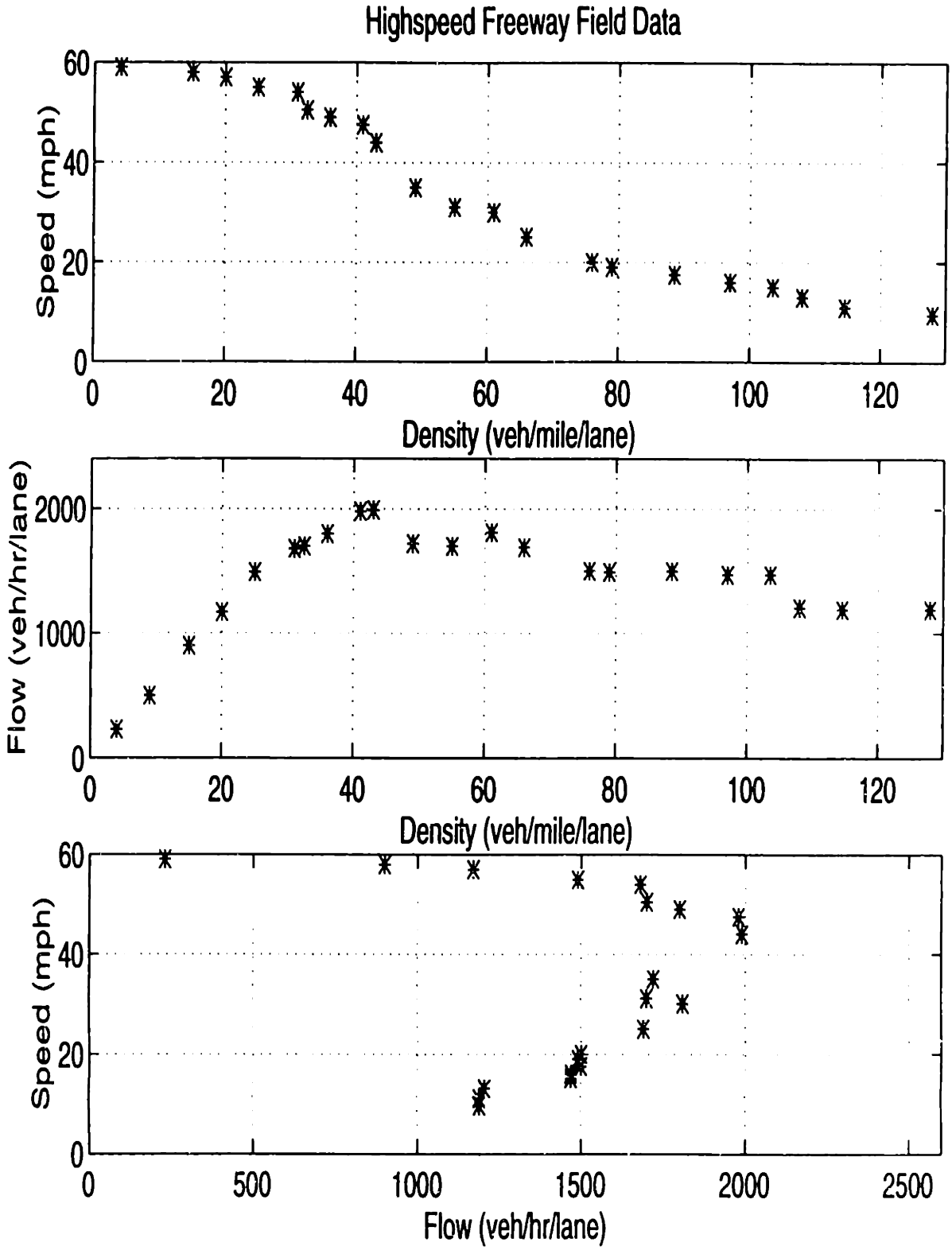

Figure 3.2: Field observations of freeway flow-speed-density relationships (Source:[29])

3.3 Validation of Flow-Speed-Density Relationships

3.3.1 Simulation Design

Based on the findings of lane loading capacity in Section 3.2, we have designed a simulation scenario for testing the basic relationships between simulated speed, flow, and density from MITSIM. The scenario is implemented using the same 3-mile two-lane freeway section that we checked for critical capacity. The total simulation time is 2 hours, starting from 7:15 am, and ending at 9:15 am. Data from both the first and last 15 minutes are discarded; the first 15 minute interval is used as a "warm-up" period, and the last 15 minute interval is used to ensure a persistent traffic pattern.

The OD flow is designed to mimic a morning peak, which progressively increases from a very small flow to an equivalent of 1,600 veh/hr/lane, then drops gradually in a similar pattern in the remaining one hour, as shown in Figure 3.3.

To get a large range variation of the simulated speed, and density, we also design an incident, taking place around 8:15 am, and lasting 25 minutes, at the location of 0.2 mile toward the end of the left lane. The incident is assumed to cause significant drop of capacity, and to result in a moving speed of 0 in the blocked lane.

The simulated network is equipped with sensors, each 528 ft apart, for monitoring traffic counts, speed, sensor occupancy, and other information. The simulated sensor outputs are sampled every 2.5 minutes. Again, to reduce the random effect of simulation seeds, 10-run averaged outputs are used in the calculations of speed, flow, and density relationships.

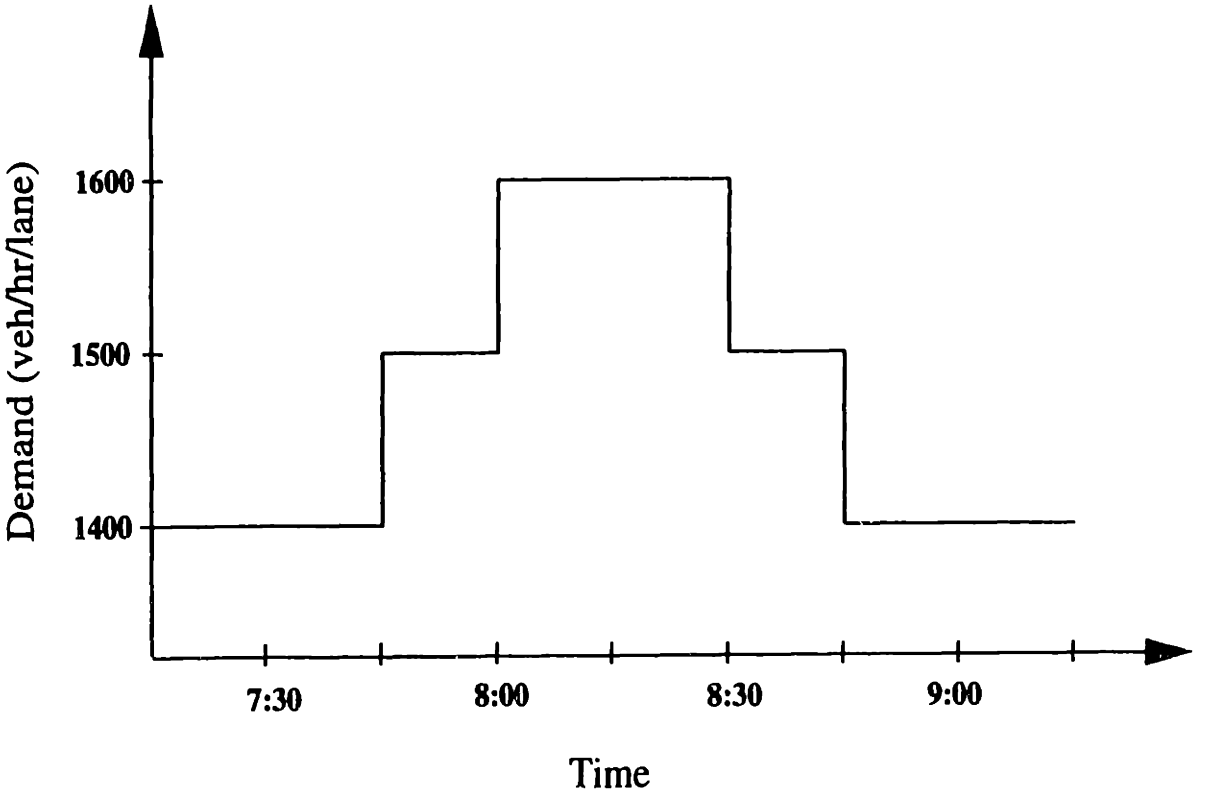

Figure 3.3: OD flow used in the validation test

3.3.2 Simulation Results

Results from sensor station 12 and 14, which locate around the middle of the network, have been selected to represent the macroscopic traffic conditions. The simulated relationships from the sensor station are shown in Figure 3.4 and 3.4.

From the figure, we observe that:

- Similar to the field data, the sample data provides a distribution of density from near 20 veh/mile/lane to 130 veh/mile/lane.

- Analogous to field observations, the simulation speed-density plot also displays a clear data pattern, and displays a slightly S-shaped relationship.

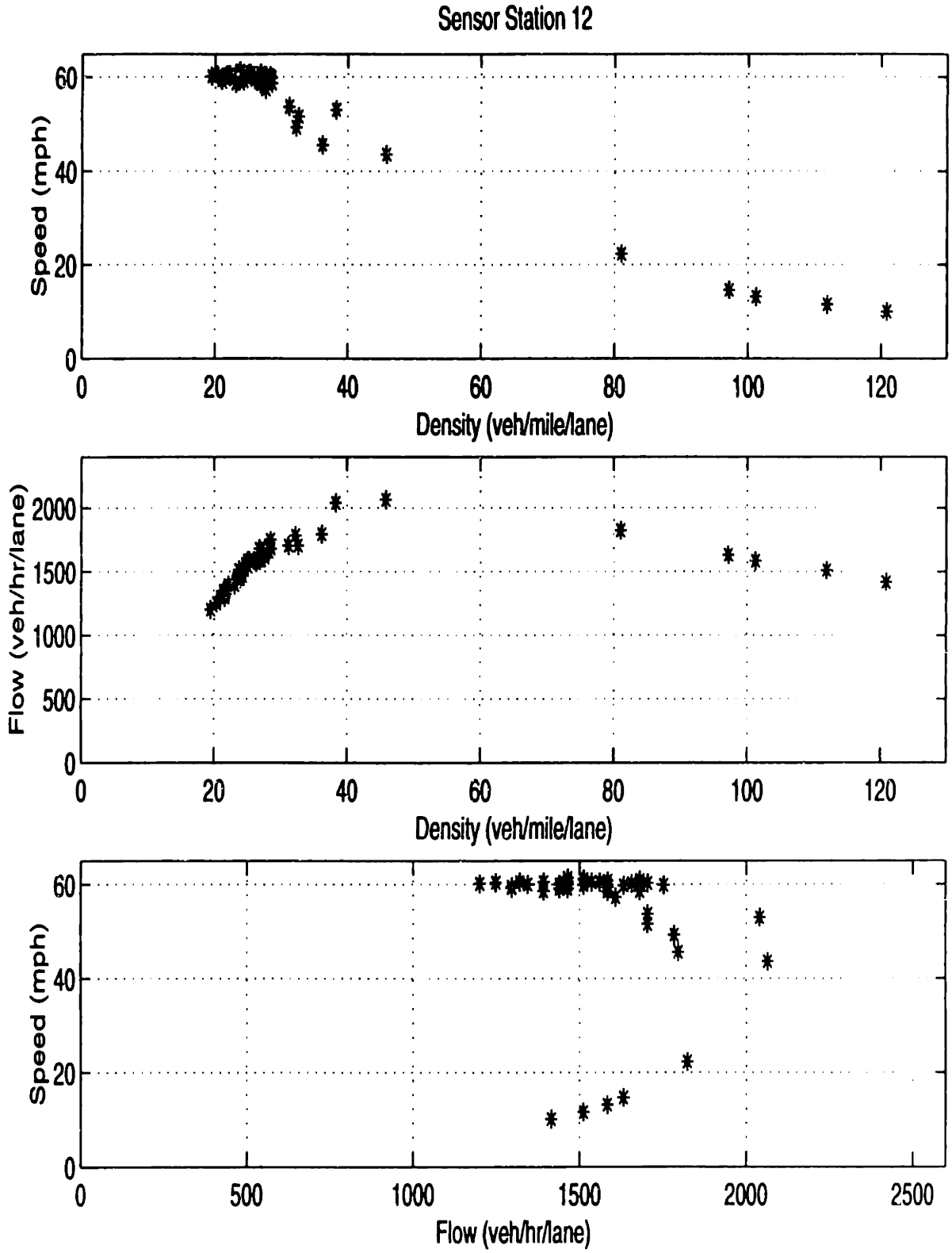

Figure 3.4: Simulation results from sensor station 12

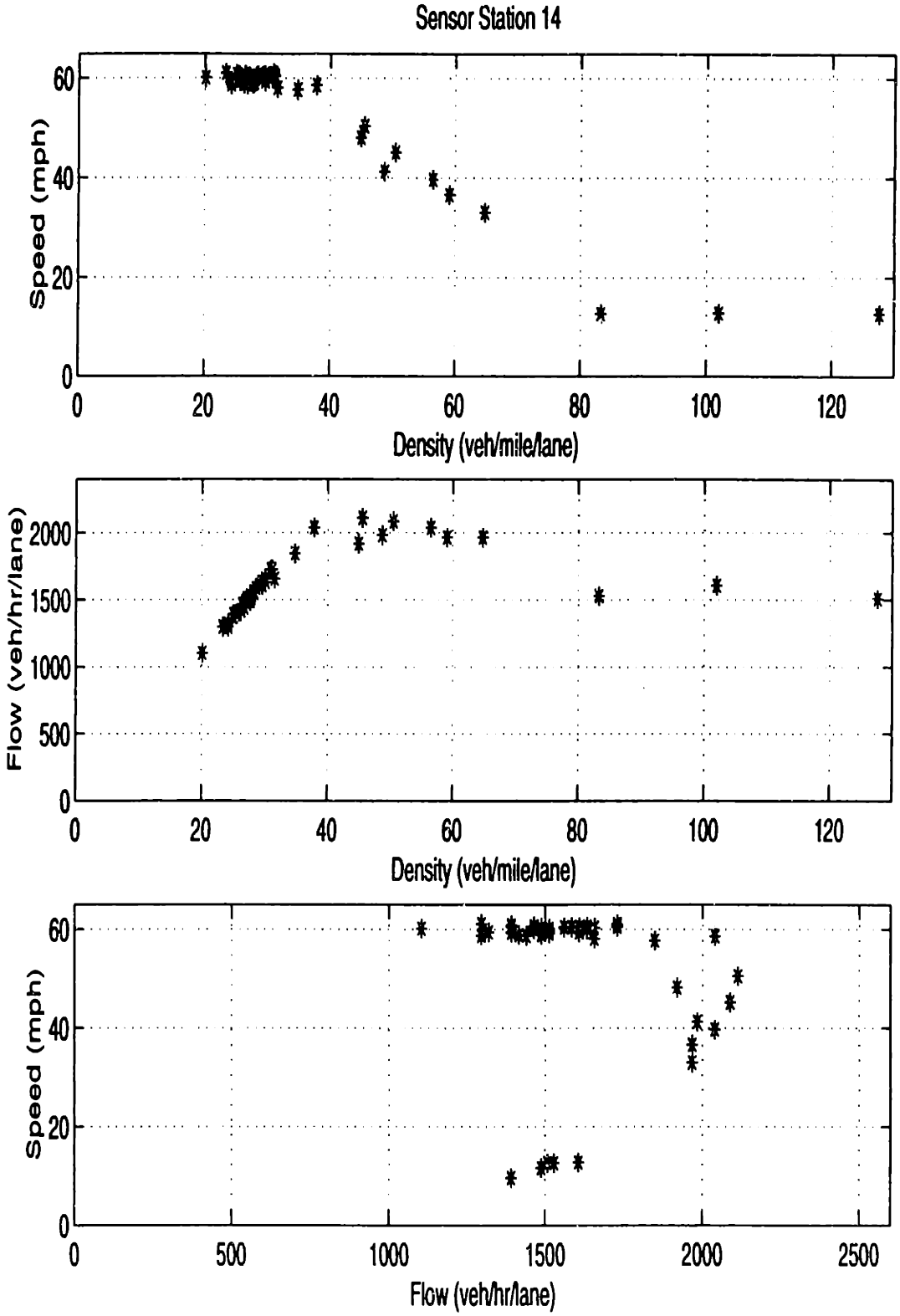

Figure 3.5: Simulation results from sensor station 14

- The free-flow speed appears to be slightly over 60 mph, but the jam density cannot be determined.

- The maximum flow or capacity, appears to be on the order of 2,000 $\sim$ 2100 veh/hr/lane, very close to what we found in the previous section; and the optimum density is approximately 40 to 50 veh/mile/lane.

- Like the field observations, the flow-density plot from simulation also shows clear and similar data patterns. The free-flow portion appears like a parabola, the congested-flow portion appears relatively flat with a tail to the right.

- The flow-speed plots shows a clear data pattern similar to the field observations. As shown in this figure, the optimum speed is not well defined and can lie anywhere between 45 to 55 mph, which is about 10 mph higher than that of the field observations.

3.3.3 Validation Findings

Comparing simulation results with field observations, we find the simulated results match those from the field reasonably well.

We make the following observations on them:

- The relationships calculated from MITSIM sensor outputs resemble the field macroscopic relationships reasonably well. The shapes of speed-density, flow-density, and flow-speed curves are all similar to the patterns displayed by the field data. The

key parameters that determine the operations of a freeway, such as maximum capacity, optimum density, free-flow speed, are very close to the field observations.

- The simulated density displays similar variability as those in the field data. It varies from about 20 veh/lane/mile to 130 veh/lane/mile. Although density lower than 20 veh/lane/mile is not observed in the simulation, it is resulted from the OD design, which start from a relative high flow of 1400 veh/hr/lane.

- The simulated speed pattern is very similar to that of the field. It ranges from less than 20 mph to a little bit higher than 60 mph. However, as we have seen from the flow-speed plot, the optimum speed from the simulation seems to be 10 mph higher than that observed in the field.

3.4 Summary

In this chapter, we first tested the vehicle loading capacity of MITSIM. By changing the OD flow rate and searching for the amount of demand that begin to cause queues, we found that $2,000 \sim 2,100$ *veh/hr/lane* can be accepted as the critical capacity. This is consistent with field observations documented in other work.

Based on this finding, we then designed a simulation scenario for validating the flow-speed-density relationships. Compared to the data collected from a California freeway, we found that the simulation results resembled the field observed patterns reasonably well. The maximum flow, optimum density, free-flow speed, and other key parameters that determine the operations of a freeway, were consistent with the values from

the field. The slightly S-shaped speed-density relationship, the semi-parabola shaped flow-density relationship, and the shape of flow-speed relationship were similar to those found in the high-speed freeway data. They demonstrate a good overall performance of MITSIM. Still, there exist a significant range difference between the simulated and field optimum speed. Further analysis is necessary to identify the sources of the problem.

Chapter 4

Validation of MITSIM on Weaving Traffic

Weaving sections are typically the most constraining parts of the freeway system. At weaving sections, considerable lane-changing activities occur as vehicles access lanes leading to their destinations. These intense lane-changing maneuvers often create traffic turbulence, which require special treatment in the freeway design process. Therefore, it is important to test the ability of MITSIM to replicate weaving traffic patterns.

This chapter is organized as follows: In *section* 4.1, we describe the Capital Beltway weaving section, the site selected for our validation analysis. In *section* 4.2, we present field observations on flow, speed, and density, computed from the Capital Beltway data set. This is followed by MITSIM simulation of these macroscopic variables and our validation findings. In *section* 4.3, we move to the validation of weaving and non-weaving speeds, which are the key parameters that determine the level of service in weaving sections. We will present the field observations, MITSIM simulation results, and validation findings for them. In *section* 4.4, we focus on microscopic level by pre-

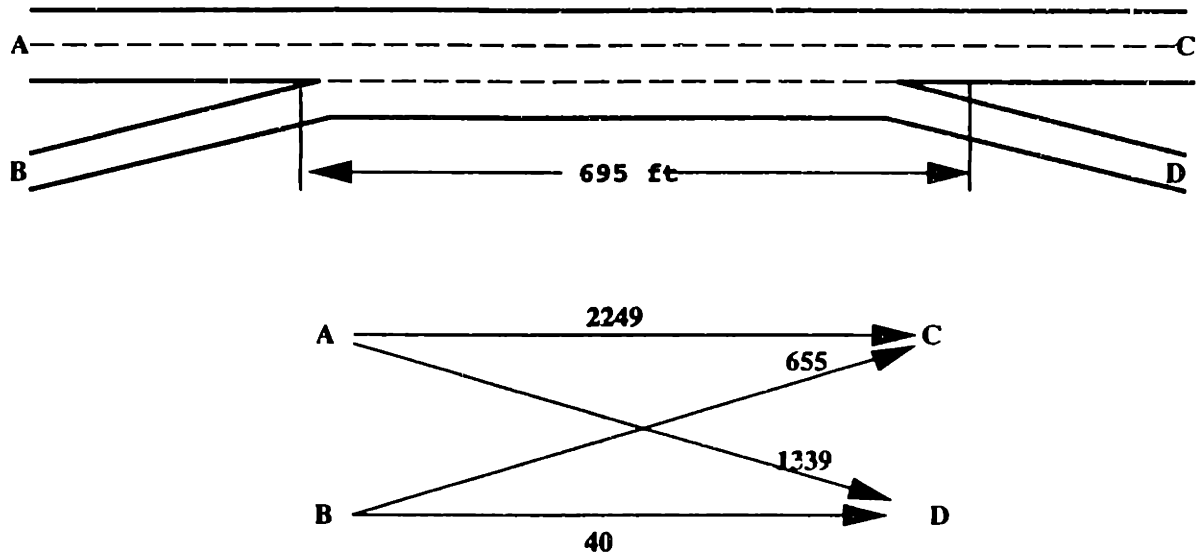

Figure 4.1: Network and Weaving Traffic Diagrams of the Capital Beltway Site

senting the field observations, MITSIM simulation results, and validation findings for headway and lane-change distributions. Finally, a summary of this chapter is presented in *section* 4.5.

4.1 Capital Beltway Weaving Section

We have chosen a ramp weaving section from the FHWA data sets as the basis for our study on weaving traffic [26]. The Capital Beltway site from Prince Georges County, MD, is a clover-leaf type weaving section. It has a total length of 1,606 feet, and a weaving length of 695 feet. Diagrams of the network and the weaving traffic are shown in Figure 4.1.

The Capital Beltway data set displays significant traffic flow variations and a great deal of lane changing activities. A total of 59 minutes of data are available. The level of service of the traffic ranges from B to C during the first 40-45 minutes, to E and F

Table 4.1: OD Flow for the Capital Beltway Weaving Section

OD	Vehicle Type						Total
	passenger car	van or pickup truck	car, van or pickup truck with trailer	single unit truck	tractor trailer truck	bus	
AC	2,135	6	6	74	28	0	2,249
AD	1,275	4	4	49	7	0	1,339
BC	633	3	0	18	0	1	655
BD	39	0	1	0	0	0	39
Unknown	15	0	0	1	0	0	16

toward the end, when short queues begin to form on the mainlines and ramp. OD flows extracted from the field vehicle trajectory data show that the majority of vehicles are passenger cars (See Table 4.1). Slightly over half of the traffic flow is in the freeway to freeway direction. Weaving traffic flow and ramp to ramp flow account for the remainder. Among the weaving traffic flow, nearly two thirds is in the freeway to off-ramp (AD) direction.

The analysis of the data has focused on the following traffic variables and their distributions: (1) OD flows, (2) spatial and temporal flow distributions, (3) spatial and temporal speed distributions, (4) spatial and temporal density distributions, (5) weaving and non-weaving speed distributions, (6) time headway distributions, and (7) lane-change distributions. Details on the computation of these variables and distributions can be found in the Appendix of this thesis.

4.2 Validation of Flow, Speed and Density

4.2.1 Field Observations

To examine weaving traffic characteristics on the macroscopic level, we have computed spatial and temporal distributions of traffic flow, density, and speed for each lane from the field data.

Flow

The spatial and temporal variations of traffic flow in each lane are shown in Figure 4.2. From the figure, we see that there exist some patterns common in the traffic flows of all three lanes. There are four evident and increasing cycles of flow, progressively changing from $1,200 - 1,400$ veh/hr/lane to about $1800 - 2,000$ veh/hr/lane. Each cycle lasts about 10-15 minutes.

Traffic flow is relatively stable along the left lane. The left lane flow increases over time, and reaches capacity (about $2,000$ veh/hr/lane) during the last 10 minutes. In the middle lane, a significant flow reduction is observed in the middle portion of the lane, near where the on-ramp joins the freeway. The flow increases over time, and reaches capacity (about $2,000$ veh/hr/lane) during the last 10 minutes. For the auxiliary lane, traffic flow displays a bulge near middle. The flow increases over time, and reaches capacity (about $1,800$ veh/hr/lane) during the last 10 minutes.

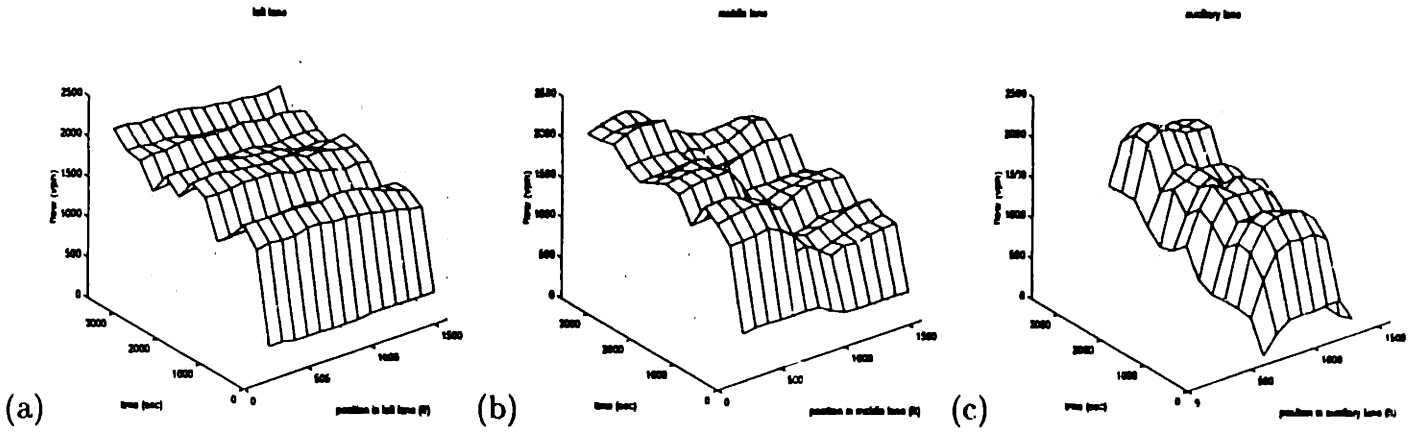

Figure 4.2: Field traffic flow distributions: (a) left lane, (b) middle lane, and (c) auxiliary lane.

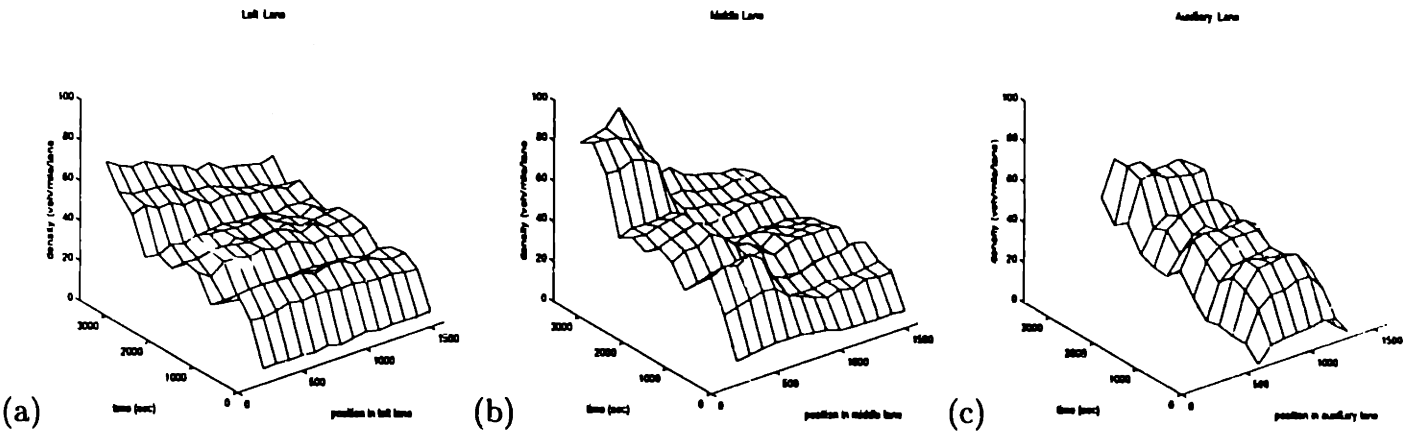

Figure 4.3: Field traffic density distributions: (a) left lane, (b) middle lane, and (c) auxiliary lane.

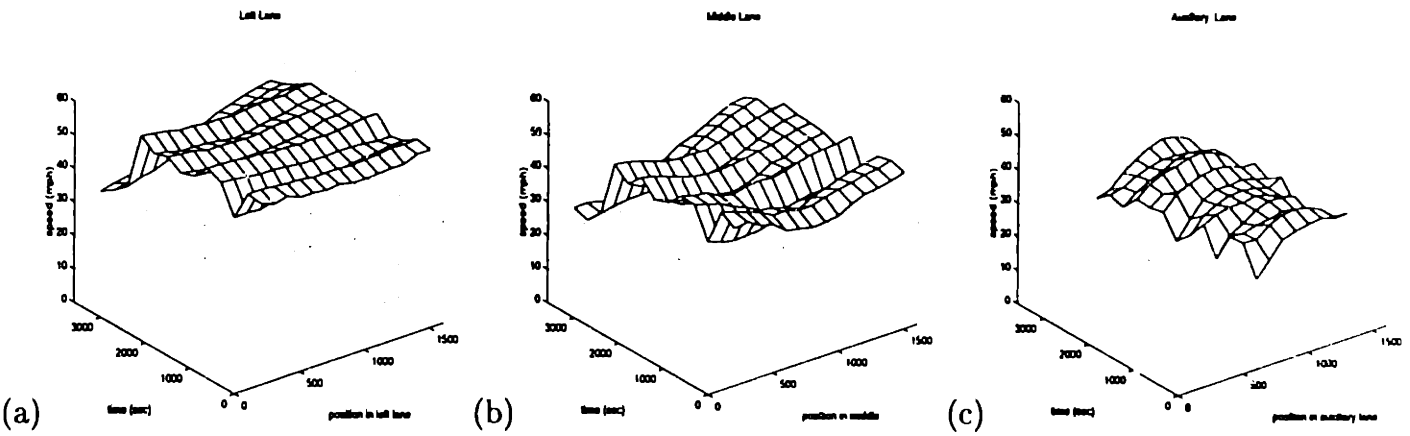

Figure 4.4: Field traffic speed distributions: (a) left lane, (b) middle lane, and (c) auxiliary lane.

Density

Density is often difficult to measure directly from the field. However, it can be calculated from the FHWA trajectory data using the following procedure: (i) we counted the number of vehicles in each snapshot (frame) for every segment of 100 ft; (ii) we average them over every 300 frames of snapshots or 5 minutes of recording time; (iii) we converted the average into vehicle/lane/mile.

The spatial and temporal distributions of traffic density in each lane are shown in Figure 4.3. They display patterns similar to the flow distributions. Common to all the lanes, there are four evident and increasing cycles of density, changing from 20-25 veh/lane/mile to nearly 60-80 veh/lane/mile, most sharply in the last cycle. Each cycle lasts about 10-15 minutes.

Along the left lane, traffic density gradually decreases. Over time, traffic density in the left lane increases, most sharply during the last cycle, in the upstream part of the lane. In the middle lane, a significant density drop is observed right around where the on-ramp joins the freeway. The density increases over time, most sharply during the last cycle, in the upstream part of the lane. For the auxiliary lane, traffic density displays a bulge in the middle. The density increases over time, most sharply in the last cycle.

Speed

The spatial and temporal distributions of traffic speed in each lane are shown in Figure 4.4. They display patterns very consistent with those of flow and density distributions. The average speeds for the three lanes are, 45 mph for the left lane, 40 mph for the

middle lane, and approximately 35 mph for the auxiliary lane.

In the left lane, traffic speed is relatively constant along the lane, although slightly lower in the middle. A sharp slowdown is observed during the last cycle, in the upstream part of the lane, where the queue occurs. Traffic in the middle lane displays a shallow "U" shape. As before, a sharp slowdown is observed during the last cycle, in the upstream part of the lane. In the auxiliary lane, the traffic speed is slightly higher in the middle, and relatively constant over time.

4.2.2 Simulation Results

At present, MITSIM does not have the capability of loading traffic flow into each lane according to some presumed proportion. The directional traffic flows have to be evenly distributed within the two mainlines. A problem with this loading mechanism is that too many simulated FR vehicles are moving in the left lane of the network until they reach the weaving section. To fix this problem, we have added 500 feet to the beginning of the network, and set up two "virtual" lane-use signs to simulate drivers' familiarity to the system. We assume these signs have view distances of 1,000 feet, so that drivers from the freeway can see the message signs and make their desired discretionary lane changes prior to entering the network. We have also added 500 feet to the end of the network in order to ensure a smooth traffic movement to the end.

The traffic flow, density and speed of each lane have been computed from simulation outputs using the current parameter set without any calibration. The results are shown in Figures 4.5, 4.6, and 4.7. Comparing these figures with those of the field, we

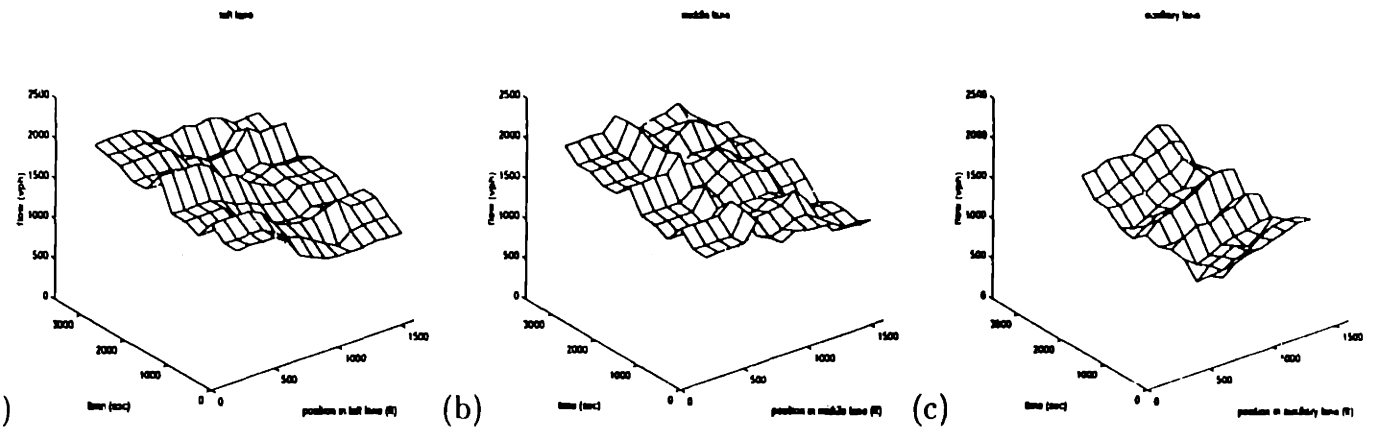

(a) (b) (c)

Figure 4.5: Simulated traffic flow distributions: (a) left lane, (b) middle lane, and (c) auxiliary lane.

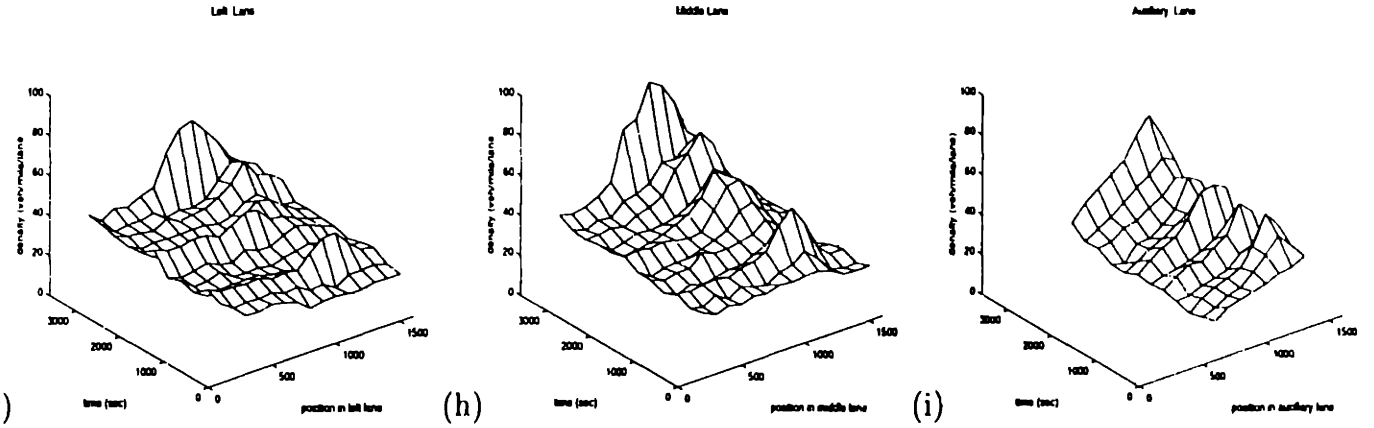

(g) (h) (i)

Figure 4.6: Simulated traffic density distributions: (a) left lane, (b) middle lane, and (c) auxiliary lane.

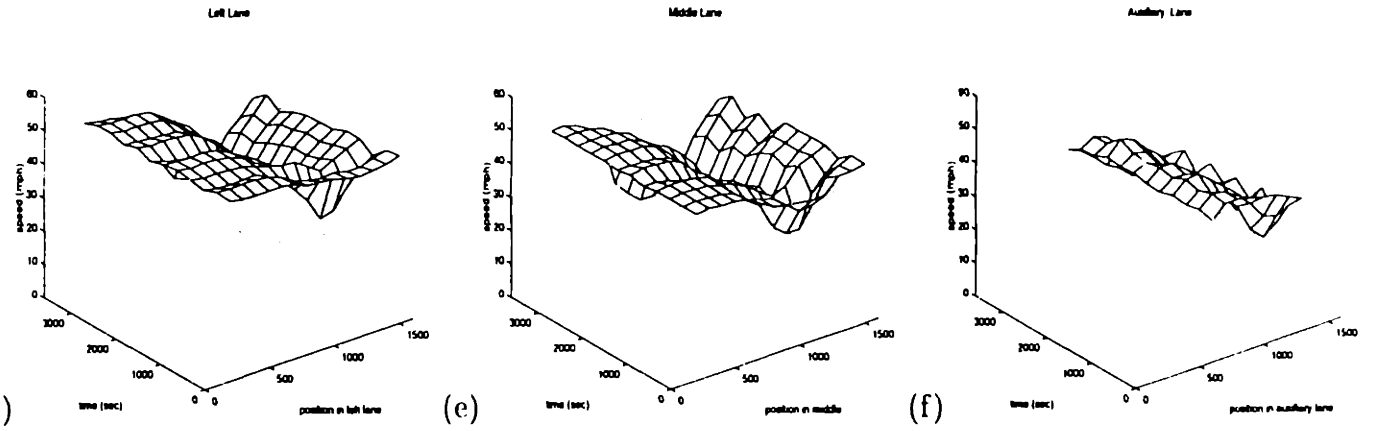

(d) (e) (f)

Figure 4.7: Simulated traffic speed distributions: (a) left lane, (b) middle lane, and (c) auxiliary lane.

find that:

1. Temporal flow cycles are observed in the simulation, which are also observed in the field data. However, the flow cycles of field data display a pattern of increase over time, which barely observed in the simulation output. In simulation, significant traffic flow reduction is observed in the left lane, whereas in the field, significant flow reduction is observed mainly in the middle lane.

2. Significant density cycles that increase over time in the simulation are also reflected in the field data. However, in simulation, the weaving traffic causes a significant increase in density around $500 \sim 600$ ft, which is not observed in the field. In the field, a significant increase in traffic density occurs around position of 800 ft in the weaving area, which is much more upstream than predicted by MITSIM.

3. Significant speed drops are observed in the simulation for all three lanes near the middle portion of the weaving area. By contrast, the slowdown is much less dramatic for field data. Moreover, the simulated speed is pretty much constant over time for all three lanes. In the field, traffic speed drops off sharply in the last 10 minutes for the two mainline lanes.

4.2.3 Validation Findings

To evaluate MITSIM's simulation performance quantitatively, we have calculated root mean square (RMS) error, RMS percentage error, correlation coefficient ρ, Theil's inequality coefficient U, bias U^M, and variance U^S, from simulated vehicle trajectory data

Table 4.2: MITSIM Performance Evaluation (Flow, Speed, and Density)

Performance Measure	Flow	Speed	Density
RMS Error	451.70	8.20	18.02
RMS Percentage Error	0.34	0.18	0.73
Correlation Coeff. ρ	0.49	0.37	0.14
Theil's Coefficient U	0.14	0.09	0.24
Bias U^M	0.00	0.07	0.02
Variance U^S	0.33	0.00	0.13
Covariance U^C	0.67	0.93	0.85

using field measurements. Details on their calculations can be found in the Appendix.

From Table 4.2, we get a mixed signal on how well MITSIM performs in simulating traffic flow, speed, and density. The RMS percentage error measure is significant for flow (0.34), and very high for density (0.73), which indicates that MITSIM cannot simulate traffic density very well. The correlation coefficient is low for speed (0.37), and very low for density (0.14), which means that speed and density are not being simulated well also. However, the Theil's inequality coefficients are low for flow, speed, and density, which would imply that the simulator is doing a good job on them. Likewise, the small biases and variances (except for the speed variance) are supportive of the same conclusion.

One possible explanation for the inconsistency between the performance measures could be that the simulation outputs appear to be a similar but shifted version of the observed traffic. By examining the figures of field data and the figures of simulation outputs, we notice that the weaving activities predicted by MITSIM are too concentrated in the middle portion of the weaving area. The dramatic density increases and speed

drops predicted by MITSIM in Figures 4.6, 4.7, occur much earlier in the field data (see Figures 4.3, 4.4). This seems to suggest that in reality, freeway to freeway (FF) and freeway to ramp (FR) traffic may change lanes early in order to avoid weaving turbulence.

4.3 Validation of Weaving and Non-Weaving Speeds

4.3.1 Field Observations

To examine the weaving traffic more closely, we break down the traffic flow by OD directions, and compute temporal distributions of traffic speed for each direction from the field data. The results are shown in Figure 4.8(a). Next, we aggregate the observations into weaving and non-weaving directions, and calculate weaving and non-weaving speeds. These results are shown in Figure 4.8(b). Details on these computations can be found in the Appendix.

As shown in Figure 4.8(a), vehicles originating from the freeway move faster than those originating from the on-ramp. Traffic in the direction of AC (freeway to freeway) is the fastest, with a mean speed of 44.51 mph, and a standard deviation of 5.69. The second fastest is in direction of AD (freeway to off-ramp), with a mean speed of 39.74 mph and a standard deviation of 5.06. Traffic flow in the BC direction (on-ramp to freeway) moves with a mean speed of 37.86 mph and a standard deviation of 2.56. Traffic flow in the direction of BD (on-ramp to off-ramp) moves the slowest, with a mean speed of 33.98 and a standard deviation of 3.66. We note that there are gaps of missing data in several time intervals of Figure 4.8(a).

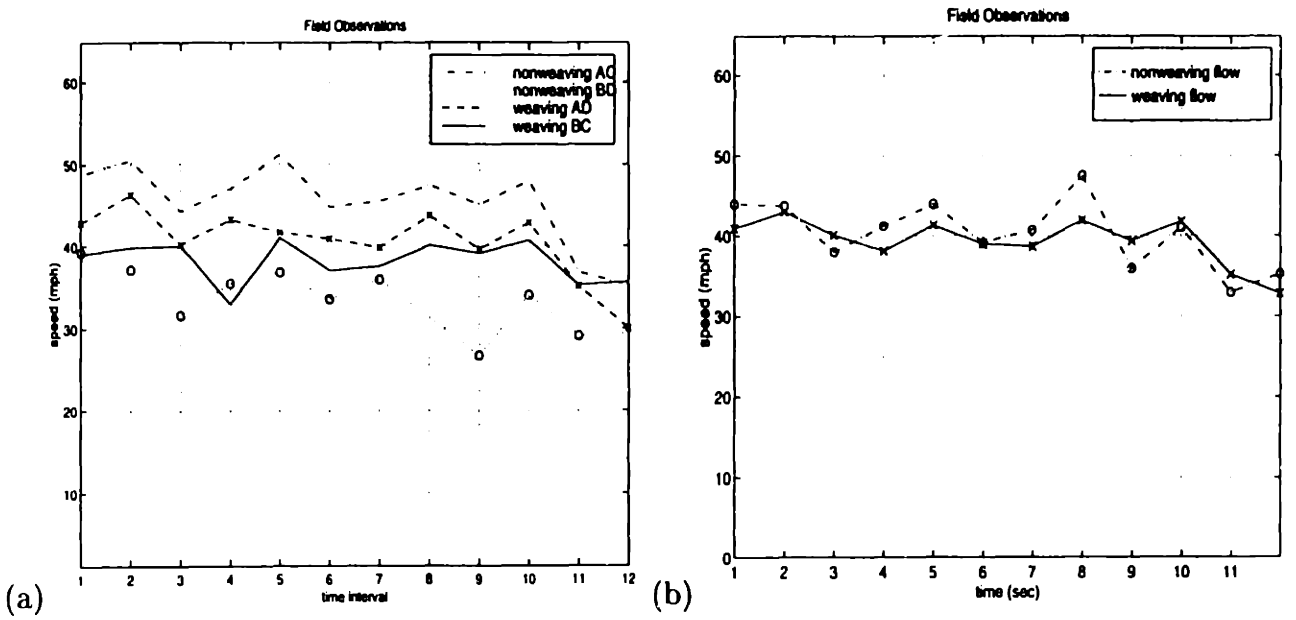

Figure 4.8: Field observations of weaving and non-weaving speeds: (a) speeds for each traffic flow direction, and (b) speeds for weaving and non-weaving traffic flows.

We observe that traffic speeds for the two weaving directions (AD and BC) are very close to each other, but the speeds for the two non-weaving directions (AC and BD) are very different. The speed in BD direction is about 10 mph slower than that of the other non-weaving direction AC. The difference in the two non-weaving speeds reflects the different speed limit set for each lane, 55 mph for the freeway, and 35 mph for the ramps. Since the weaving traffic moves from one speed limit to another, it effectively produces an averaging of the two speed limits.

We also notice that traffic speeds for the four directions all drop significantly as traffic flow increases to level of service F in the last 10 minutes. It seems that the faster moving lanes are most affected by the slowdown, whereas the slower moving lanes are less affected. Due to these effects, we see a narrowing of the range between the component speeds, or a convergence toward a uniform breakdown speed.

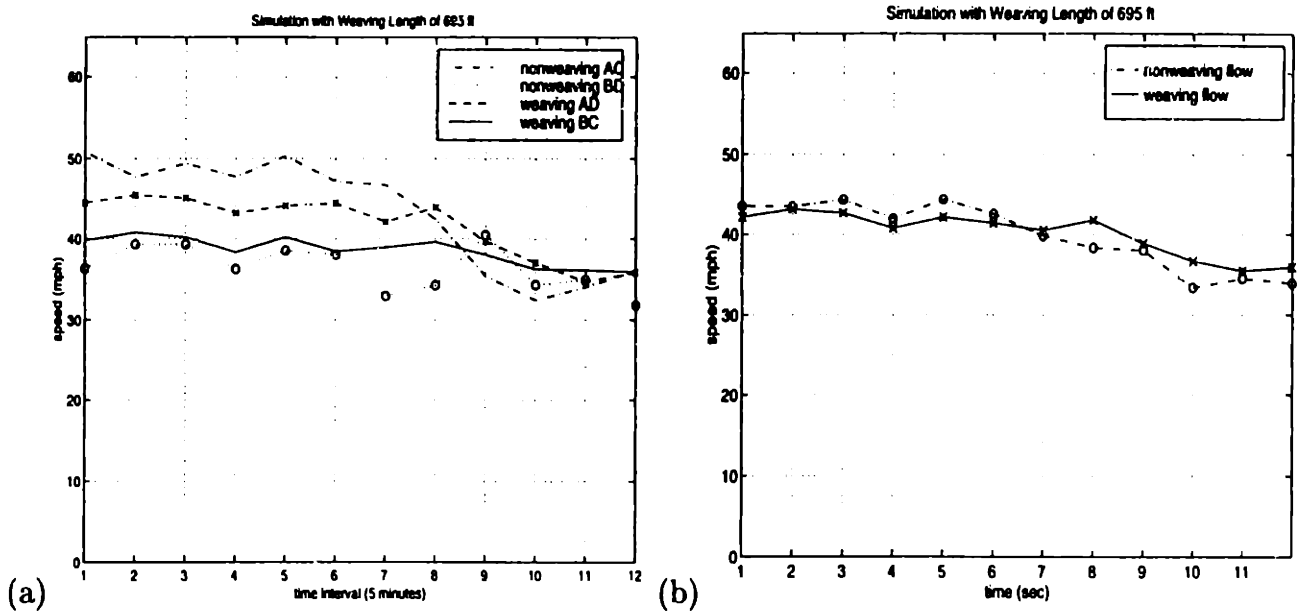

Figure 4.9: Simulation results of weaving and non-weaving speeds: (a) speeds for each traffic flow direction, and (b) speeds for weaving and non-weaving traffic flows.

From Figure 4.8(b), we see that the speeds of weaving and non-weaving traffic are very close to each other. The mean weaving speed is about 38.80 mph, and the mean non-weaving speed is about 39.53 mph. Speed drops are observed for both weaving and non-weaving vehicles in the last ten minutes. A converge value of 35 mph (breakdown speed) between the two flows is also observed during this time interval.

4.3.2 Simulation Results

Simulated trajectory data, have been processed to compute average speeds for the four traffic flow directions, and average speeds for weaving and non-weaving traffic flows. The results are shown in Figure 4.9. The simulation was run using the same parameter set as before without any calibration.

Table 4.3: MITSIM Performance Evaluation (Weaving and Non-Weaving Speeds)

Performance Measure	Non-Weaving Speeds			Weaving Speeds		
	AC	BD	combined	AD	BC	combined
RMS Error	5.90	6.57	4.14	3.15	2.20	2.27
RMS Percentage Error	0.13	0.20	0.10	0.09	0.06	0.06
Correlation Coeff. ρ	0.60	0.68	0.75	0.82	0.88	0.87
Theil's Coefficient U	0.04	0.05	0.04	0.04	0.05	0.04
Bias U^M	0.24	0.05	0.02	0.13	0.00	0.02
Variance U^S	0.19	0.28	0.01	0.02	0.07	0.06
Covariance U^C	0.57	0.67	0.97	0.85	0.93	0.92

Comparing the figures with those of the field results, we find that the speed predictions for the four component flows are very similar to the field observations. They display the same kind of ordering by direction, as well as the convergence pattern toward a breakdown speed in the last ten minutes. However, the predicted speed variations appear to be smoother and less noisy than the field observations. The speed predictions for the weaving and non-weaving flows also seem to be in good match with the field observations.

4.3.3 Validation Findings

To evaluate MITSIM's simulation performance quantitatively, we have calculated root mean square (RMS) error, RMS percentage error, coefficient of correlation ρ, Theil's coefficient U, bias U^M, and variance U^S from simulated vehicle trajectory data and field measurements. The results are given in Table 4.3.

The performance measures show decent simulation results for every flow category.

The RMS percentage error is quite low except for the BD direction (0.20). The correlation coefficient is higher for weaving speeds (0.87 vs. 0.75). Theil's inequality coefficient is very high for every flow category, which suggests the existence of systematic biases. Component flow speeds that appear to have significant bias include the AC direction (0.24) and the AD direction (0.13). Component flow speeds that appear to have significant variance include the AC direction (0.19) and the BD direction (0.28).

Overall, non-weaving speeds are not simulated as well as weaving speeds. There are at least two reasons for this. First, the field observations for non-weaving BD direction are few and sporadic. Second, in field observations, there are many drivers who make irrational lane changes, for instance, changing from the on-ramp to the freeway then to the off-ramp. These drivers tend to increase the variance of the field data, and create traffic turbulence. However, in MITSIM drivers are modeled as standard commuters familiar with the network. Real world drivers tend to be more unpredictable and erratic than simulated drivers.

4.4 Validation of Microscopic Behavior

In our analysis of car-following and lane-changing behavior, we have separated vehicles into two categories: vehicles that remain in the same lane, and vehicles that change lanes. Car-following behavior or headway distributions are only analyzed for those vehicles that do not change lanes.

4.4.1 Field Observations

We have a total of 10,260 headway samples from the field. Headway distributions for all three lanes of the Capital Beltway weaving section have been computed from the field data, and are plotted in Figure 4.10. The mean and standard deviation of the headway distribution for each lane have also been calculated. Using the regime thresholds of the MITSIM car-following model, (h_{upper} = 1.36 seconds and h_{lower} = 0.50 seconds), we have computed the frequency of field headway samples in various regimes. These statistics are shown in Table 4.4.

The mean of all time headways observed in the field is 2.32 seconds, and the standard deviation 2.05 seconds. The majority (65%) of the headways in the samples fall in the free-flow regime, followed by 34% in the car-following regime, and only 1% in the emergency regime.

The headway distributions of the two freeway lanes (left and middle lanes) look similar to each other, except for their tails. The middle lane has a bigger tail than the

Table 4.4: Statistics of Field Headway Distributions

Lane	Mean	Std	Emergency Regime (h<0.50)	Car-Following Regime (0.50≤h≤1.36)	Free-Flow Regime (h>1.36)	Total Number of Observations
left lane	1.99	1.67	1%	39%	60%	6827
middle lane	2.99	2.55	1%	23%	75%	3316
auxiliary lane	2.99	1.86	1%	12%	87%	115
lanes combined	2.32	2.05	1%	34%	65%	10260

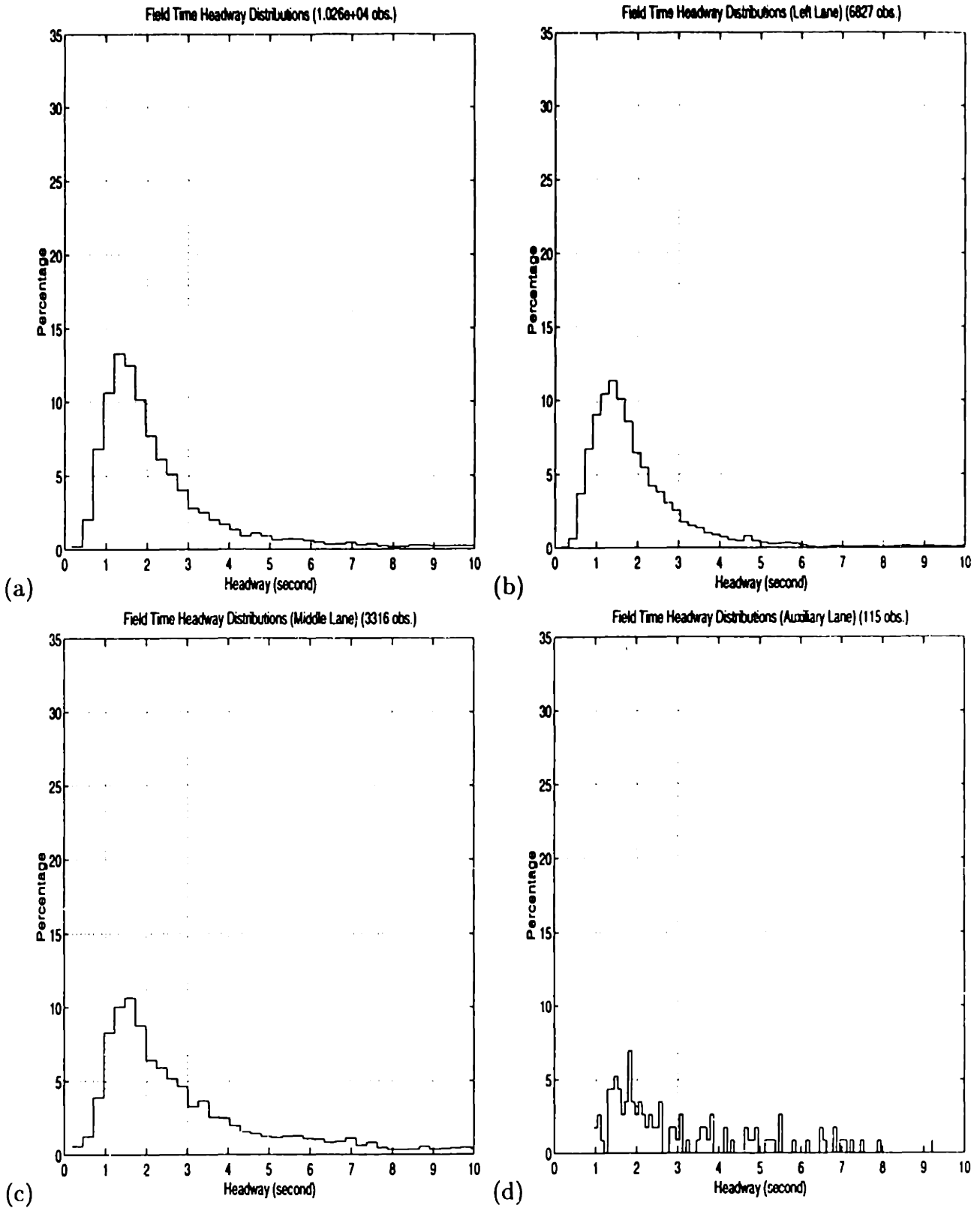

Figure 4.10: Field headway distributions: (a) combined distribution of the three lanes, (b) left lane, (c) middle lane, and (d) auxiliary lane.

left, and this is reflected by the greater percentage of middle lane headways to fall in the free-flow regime as compared to the left lane (75% versus 60%). Therefore, it is not surprising that on average, vehicles in the middle lane have longer time headways than the left, 2.99 seconds as compared to 1.99 seconds. This is expected since lane-changing activity is more intense in the middle lane than in the left lane, and vehicles may maintain higher headways.

Compared to the two freeway lanes, the auxiliary lane is more similar to the middle lane than to the left lane, both in terms of the headway mean, and the headway distributions in various regimes. The mean of the auxiliary lane is identical to that of the middle lane, 2.99 seconds, and the auxiliary lane has the highest percentage of headways in the free-flow regime, 87%, followed by the middle lane with 75%. The statistics suggest that lane-changing activity may also be quite intense in the auxiliary lane.

4.4.2 Simulation Results

To check the validity of MITSIM car-following model, we now discuss the headway distributions from simulation data (See Figure 4.11). The simulation was run using the same parameter set as before without any calibration. The mean and standard deviation for headway distribution of each lane have also been calculated. Using the same regime thresholds of the MITSIM car-following model as before, we have computed the frequency of simulated headway samples in various regimes. These statistics are shown in Table 4.5.

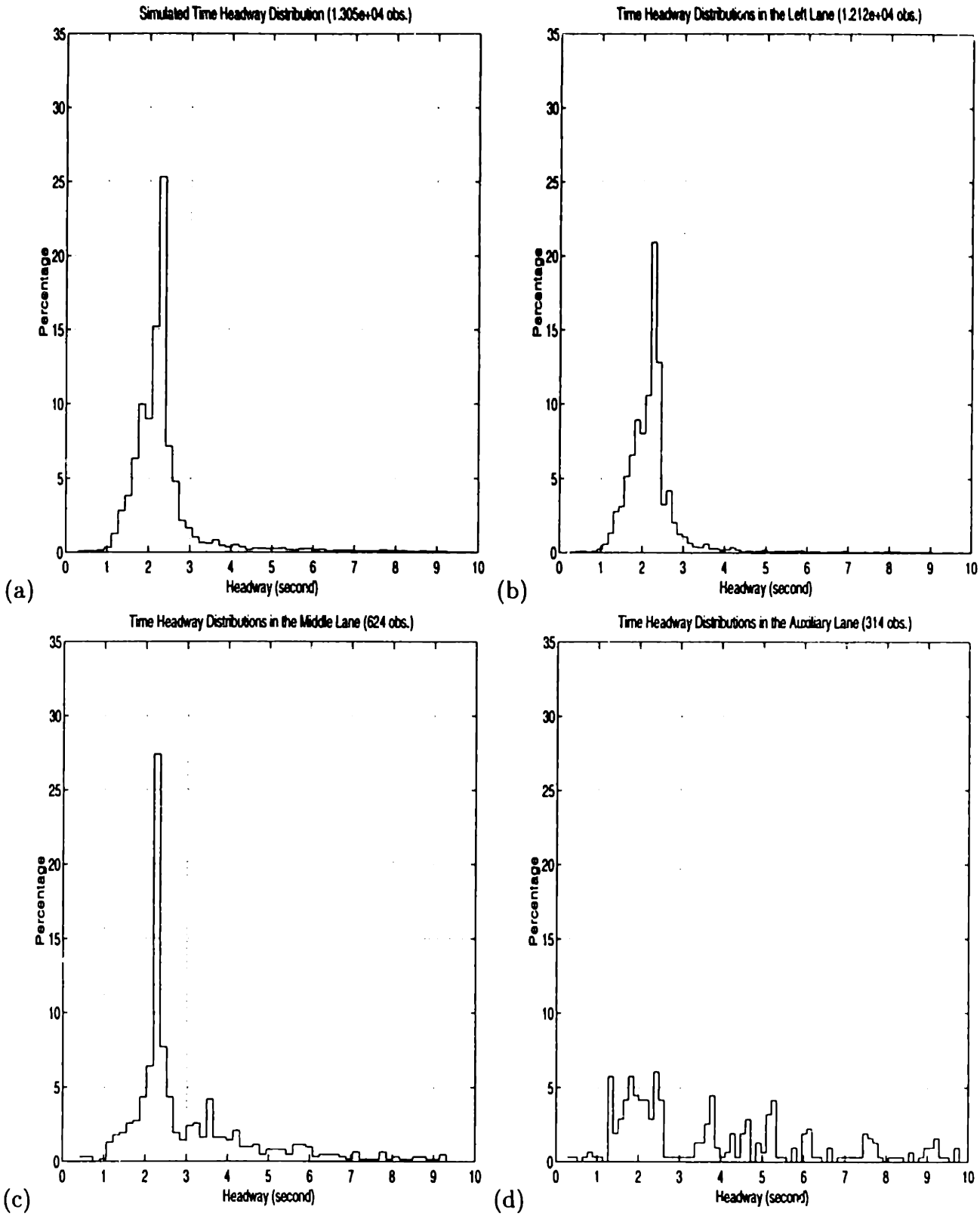

Figure 4.11: Simulated headway distributions: (a) combined distribution of the three lanes, (b) left lane, (c) middle lane, and (d) auxiliary lane.

Table 4.5: Statistics of Simulated Headway Distributions

Lane	Mean	Std	Emergency Regime (h<0.50)	Car-Following Regime (0.50≤h≤1.36)	Free-Flow Regime (h>1.36)	Total Number of Observations
left lane	2.27	1.08	0%	5%	95%	12120
middle lane	3.17	2.08	0%	5%	95%	624
auxiliary lane	3.83	2.48	1%	8%	91%	314
lanes combined	2.36	1.23	0%	5%	95%	13050

Comparing the figures and the table with those from the field, we observe a number of differences. First, the simulated distributions are quite different from field distributions. The peaks of all simulated distributions are higher than those of field distributions, and appear to be shifted by one second to the right.

The next major difference is that the simulated distributions are much more localized around their peaks than the field distributions. As a result, a smaller overall standard deviation (1.23 seconds for simulated data versus 2.05 seconds for field data) is observed in the simulated data. It seems that nearly all of the simulated headway samples fall under the free-flow regime 95% as compared to 65% for field headway samples.

Third, the pattern of change over the three lanes is somewhat different from that of the field data. The field data show progressive increases in headway mean and the percentage of headway samples in free-flow regime, as we move from the left lane, through the middle lane, to the auxiliary lane. The simulated data display the same pattern of increase in the value of the mean, but the pattern of change of the percentage of headways

falling under free-flow regime is different.

4.4.3 Validation Findings

After a further investigation of the differences between field headway distributions and simulated headway distributions, we reach the following conclusions:

- MITSIM tends to be more conservative and predicts longer headways for all three lanes.

- MITSIM predicts a smaller variability of headway than that observed in the field. This finding appears to be consistent with the validation findings for weaving and non-weaving speeds, where we have suggested that in MITSIM, drivers are modeled as standard commuters familiar with the network. As a result, the simulated data all fall within much narrower ranges than those from the field.

- Given the regime thresholds defined by the MITSIM car-following model, fewer simulated headways are in the car-following regime as compared with those in the field. Correspondingly, more simulated headways are in the free-flow regimes. This indicates that the current headway regime of $h_{upper} = 1.36$ may be too high.

4.5 Validation of Lane-Change Distribution

4.5.1 Field Observations

The Capital Beltway trajectory data provides us with complete information on both the mandatory and discretionary lane-change distributions that occurred in this weaving

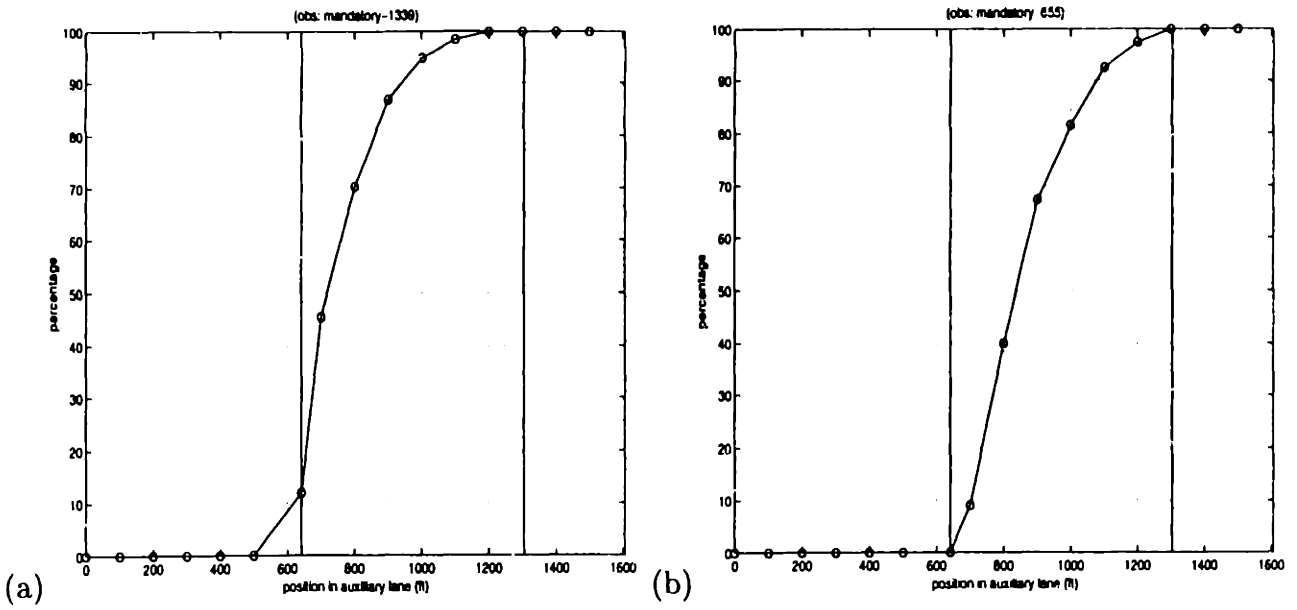

Figure 4.12: Field mandatory lane change distributions for traffic in AD and BC directions. (a) AD direction, and (b) BC direction.

section.

Mandatory Lane Change Distributions: Mandatory lane changes occur by vehicles in the AD and BC directions. Vehicles in the AD direction have to make at least one lane change from the middle lane to auxiliary lane, in order to exit the network through the off-ramp. Vehicles in the BC direction have to make at least one lane change from the auxiliary lane to the middle lane in order to enter mainline freeway and reach their destinations. The observed mandatory lane change distributions for vehicles in the AD and BC directions have been computed from field data, and are shown in Figure 4.12.

Figure 4.12(a) shows the location where vehicles in the AD direction enter the auxiliary lane from the middle lane (with solid straight lines indicating the beginning and end of the weaving section). A total of 1,339 vehicles make this type of mandatory

lane change. As we can see from the figure, most of these mandatory lane changes are executed within the first half of the weaving section, with 45% finished within the first 100 ft of the weaving section, 90% finished within the first 300 ft, and 100% finished about 200 ft before the end of the weaving section.

Figure 4.12(b) shows the location in auxiliary lane where vehicles in the BC direction leave in order to enter the middle lane. A total of 655 vehicles are observed to make this type of mandatory changes. As shown in the figure, 80% of the lane changes are executed within the first 400 ft of the weaving section, and only 5% of the lane changes are observed to take place near the end of the weaving section.

Discretionary Lane Change: In the Capital Beltway network, most of the discretionary lane changes occur between the middle lane and the left lane of the freeway. Since weaving traffic causes a lot of speed disturbance for the middle lane, some vehicles in the AC direction elect to make discretionary lane changes, moving from the middle lane to the left, to avoid the disturbance and attain higher speed. Although discretionary lane changes may also happen in other directions, the lane changes in the AC direction are the most important. The pattern of discretionary lane change has been calculated from field data and is shown in Figure 4.13.

We observe 277 lane changes from the middle lane to the left lane, executed by vehicles traveling in the AC direction. This type of discretionary lane changes distribute relatively evenly along the freeway, with a sharp increase in the weaving section. About 70% of the lane changes are executed in the weaving section, only 10% executed upstream

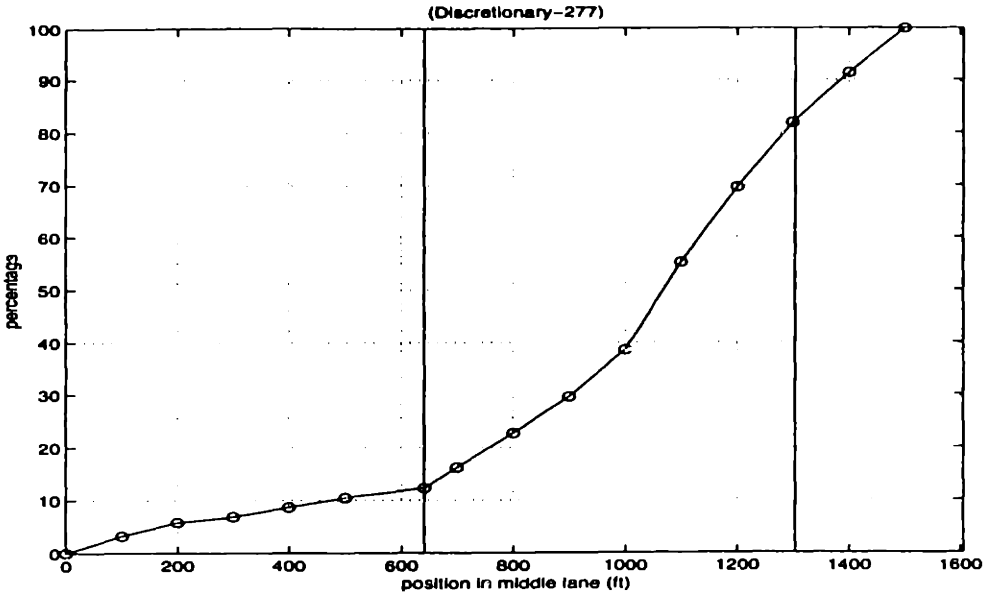

(a)

Figure 4.13: Field discretionary lane change distributions for traffic in AC direction.

of the section, and the remaining 20% executed downstream of the section.

4.5.2 Simulation Results

To examine the performance of MITSIM lane-changing model, we have computed corresponding distributions of mandatory and discretionary lane changes. They are shown in Figures 4.14 and 4.15.

In MITSIM simulation, vehicles in the AD direction have been observed to make 1,282 mandatory lane changes. Nearly 60% of the mandatory lane changes take place around the on-ramp junction. Approximately 80% of the lane changes are executed before the first 100 ft of the weaving section. In the BC direction, 618 mandatory lane changes have been observed in the simulation. More than 50% of the BC vehicles change their lanes at the on-ramp junction. Nearly 70% of the lane changes are executed before the first 100 ft of the weaving section. The simulation was run using the same parameter

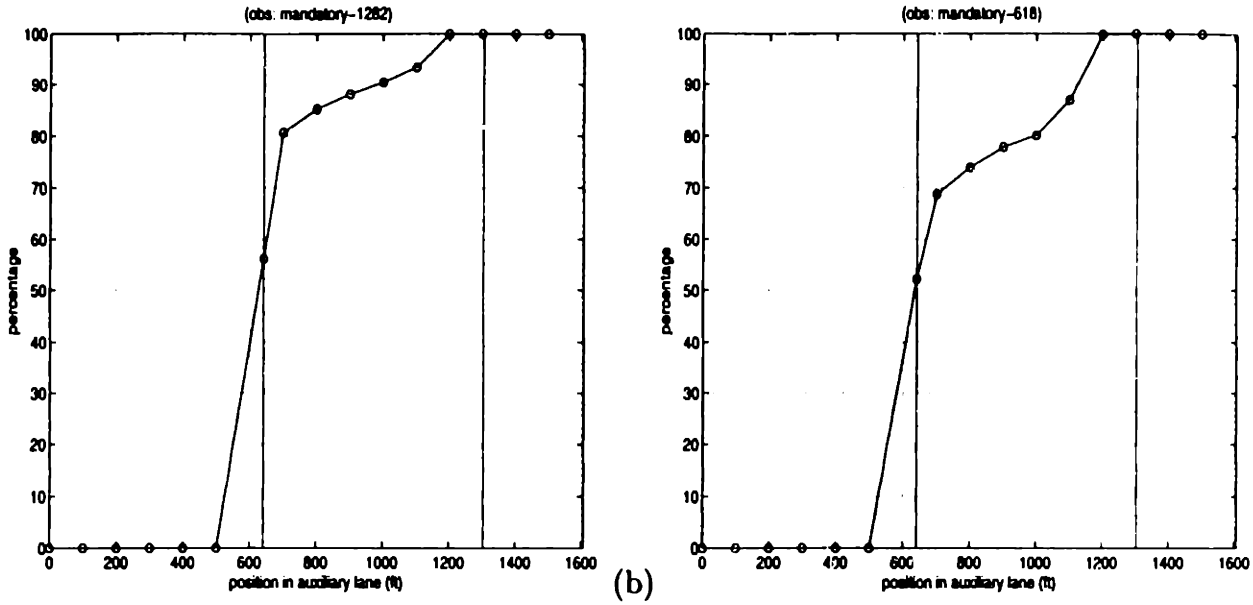

Figure 4.14: Simulated mandatory lane change distributions for traffic in AD and BC directions. (a) AD direction, and (b) BC direction.

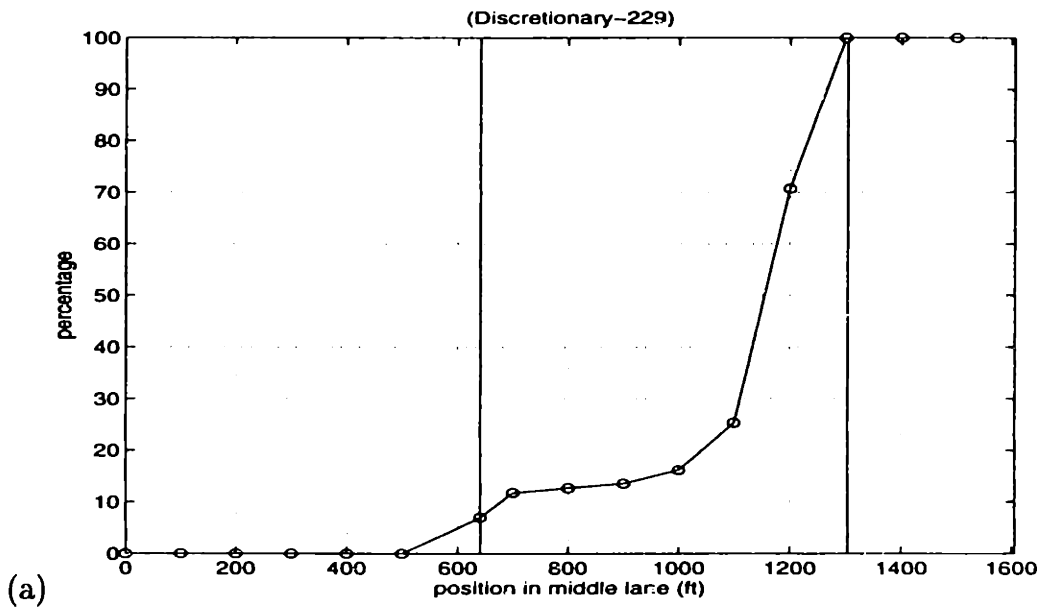

Figure 4.15: Simulated discretionary lane change distributions for traffic in AC direction.

set as before without any calibration.

Figure 4.15 shows the simulated discretionary lane-change distributions. For vehicles in the AC direction, 229 discretionary lane changes, moving from the middle lane

to the left lane, have been observed. Only 25% of the lane changes take place within the first 400 ft of the weaving section. Most of the changes take place around the last 300 ft of the weaving section.

4.5.3 Validation Findings

Comparing simulated distributions with those from the field, we find:

- Compared with field observations, the simulated mandatory lane changes tend to be "concentrated" around the on-ramp junction. This extreme lane change pattern may cause significant speed drop around the location, and may account for the sharp slowdown of speeds in the middle and auxiliary lanes we have observed in the previous lane speed comparison.

- The number of simulated discretionary lane changes is also slightly lower than that observed in the field. There are two possible causes for this: (i) a possible under-estimation of the weaving flows used in the simulation, and (ii) vehicles may change lanes prior to entering the network of interest in order to avoid turbulence.

- Compared with field observations, the simulated discretionary lane changes tend to be "concentrated" within the weaving section. This extreme lane change pattern may also cause more speed disturbance in the second half of the left lane, resulting in lower speed than that observed in the field.

Based on these findings, we suggest that future calibration work may focus on these areas: (i) Collect more field data to study the field lane-change patterns; (ii) Fit

MITSIM lane-change model to the field observations.

4.6 Summary

In this chapter, we validate MITSIM through a case study of a ramp-weaving section, the Capital Beltway network. We first present the flow, speed, and density patterns of the field data and compare MITSIM simulation results with them. Through statistical analysis, our evaluation showed MITSIM can simulate traffic flow relatively well. However, its performance with simulating lane speed and density is not as good.

Then, we examine MITSIM's performance in simulating weaving and non-weaving traffic flows. We compare the simulated component speed, and simulated weaving and non-weaving speeds with those from the field. Our validation results show that MITSIM can simulate both the weaving and non-weaving speed reasonably well, but not so well for the component flows.

Next, we validate MITSIM by comparing simulated and observed headway distributions. Our comparisons reveal that the simulated headways have a peak shift of about one-second to the right, display less deviation, have more samples in the free-flow regime, and exhibit different patterns of change across lanes. They indicate that the presumed driver reaction time may be too long, the driver behavior may be too idealized, and our current upper-bound regime parameter, h_{upper} may be too low.

Finally, we validate MITSIM on the lane-change distribution, another microscopic property. The comparison of mandatory and discretionary lane change distributions

show that the mandatory lane changes are too intensive around the on-ramp junction, while the discretionary lane changes are too intensive in the weaving area. More calibrations and testings of the lane-change model are needed.

Chapter 5

HCM Prediction and Sensitivity Analysis

In Chapter 4, we have seen that the MITSIM predictions of weaving and non-weaving speeds are quite good. We want to compare the predictive power of MITSIM with that of the HCM, which has provided a set of procedures for estimating the impact of various roadway configurations on traffic flows. The HCM procedure for analyzing Type A weaving section will be applied to the Capital Beltway network. Furthermore, to test the sensitivity of MITSIM to the geometric characteristics of the weaving section, we conduct an analysis by changing the weaving length of the original network. HCM's and MITSIM's responses to these changes will be studied by comparing their predictions of weaving and non-weaving speeds.

This chapter is organized as follows: In *Section* 5.1, the HCM procedure for predicting weaving and non-weaving speeds is presented. The procedure is then applied to the Capital Beltway network, and its predictions of weaving and non-weaving speeds are compared with field observations. In *Section* 5.2, we describe the results of testing

HCM and MITSIM on three new scenarios with different weaving lengths. Finally, the findings of the this chapter are summarized in *Section* 5.3.

5.1 HCM Predictions

The Highway Capacity Manual (HCM)[6] specifies a procedure for estimating the impact of weaving disturbances on the level of service. A suitable prediction equation is selected based on the network configuration and state of operation. The weaving and non-weaving speeds for the given scenario can be estimated by substituting traffic flow and geometry information as inputs into the equation. Level of service is determined by comparing the predicted speeds with empirical criteria given by the HCM.

The determination of whether a particular section is operating in a *constrained* or *unconstrained* state is based on the comparison of two variables: N_w - the number of lanes that are needed by weaving vehicles in order to achieve balanced or unconstrained operations, and $N_w(max)$ - the maximum number of lanes that may be used by weaving vehicles. Cases where $N_w \leq N_w(max)$ are unconstrained operations, there are no impediments to weaving vehicles using the required number of lanes. When $N_w > N_w(max)$, the configuration constrains weaving flows, which may result in a bottleneck.

5.1.1 Main Inputs

Traffic Flow: Traffic flow in a typical weaving section is composed of four component flows: freeway to freeway (FF), freeway to ramp (FR), ramp to freeway (RF), and ramp to ramp (RR). Different proportion of flow in each direction will result in different degrees

of weaving disturbance and level of service. For example, a larger portion of weaving flow will generate more lane changes, causing greater turbulence, and resulting in lower level of service. The impact of flow proportion can be measured by two variables: weaving flow to total traffic flow ratio (VR), and the ratio between two weaving flows (R).

Roadway Configuration: The roadway geometry can be represented by weaving length and weaving width. Weaving length (L) constrains the time and space in which the driver must make all mandatory lane changes. Thus, as the length of a weaving area increases, the intensity of lane-changing activity decreases and the resulting level of service increases. Width of the weaving area is measured by the number of lanes in the section. It is, however, not only the total number of lanes (N) that affects the weaving area operations, but also the proportion of lanes used by weaving and non-weaving vehicles. Therefore, the impact of weaving width is often represented by v/N.

5.1.2 Prediction Equations

In HCM, the weaving speed S_w, and non-weaving speed S_{nw}, for a Type A weaving network such as the Capital Beltway is given by the formula:

$$S_w \text{ or } S_{nw} = 15 + \frac{50}{1 + a(1 + VR)^b (v/N)^c / L^d} \tag{5.1}$$

where VR is weaving flow to total flow ratio, v is the ideal traffic flow, and N is the total number of lanes. The model constants a, b, c, and d are given in HCM.

To apply the formula, each component traffic flow (V in veh/hr) needs to be

Table 5.1: Component flows under ideal traffic conditions (*pcphpl*)

Time Interval	AC	AD	BC	BD
0 - 15 min	2376.40	1586.53	837.16	66.00
15 - 30 min	2354.36	1568.68	816.00	64.00
30 - 45 min	2344.42	1557.47	820.77	64.00
45 - 59 min	2364.00	1570.00	836.00	64.00

converted to flow under ideal traffic conditions (v in pcph) using the equation:

$$v = \frac{V}{PHF \times f_{HV} \times f_w \times f_p} \tag{5.2}$$

where PHF is peak-hour factor, f_{HV} is heavy vehicle adjustment factor, f_w is lane width adjustment factor, and f_p is driver adjustment factor.

In our calculations, we assume all drivers are familiar with the network, i.e. the driver adjustment factor $f_p = 1.0$. Since the lane width of the network is 12 feet, the lane width factor f_w is 1.0. Peak hour factor (PHF) and heavy vehicle adjustment factor (f_{HV}) are estimated every 15-minutes from the field data. The converted component flows are shown in Table 5.1.

Assuming an unconstrained operation, we can estimate N_w, the minimum number of lanes required by weaving vehicles using the equation:

$$N_w = 2.19N \times VR^{0.571} \times L_W^{0.234} / S_w^{0.438} \tag{5.3}$$

where VR is the volume ratio of weaving flow to total traffic flow, L_W is weaving length, in 100 ft, and N is the number of lanes. N_w is estimated to be on the order of $1.6 \sim 1.8$ lanes, which is higher than $N_w(max)$, the maximum number of lanes that are available

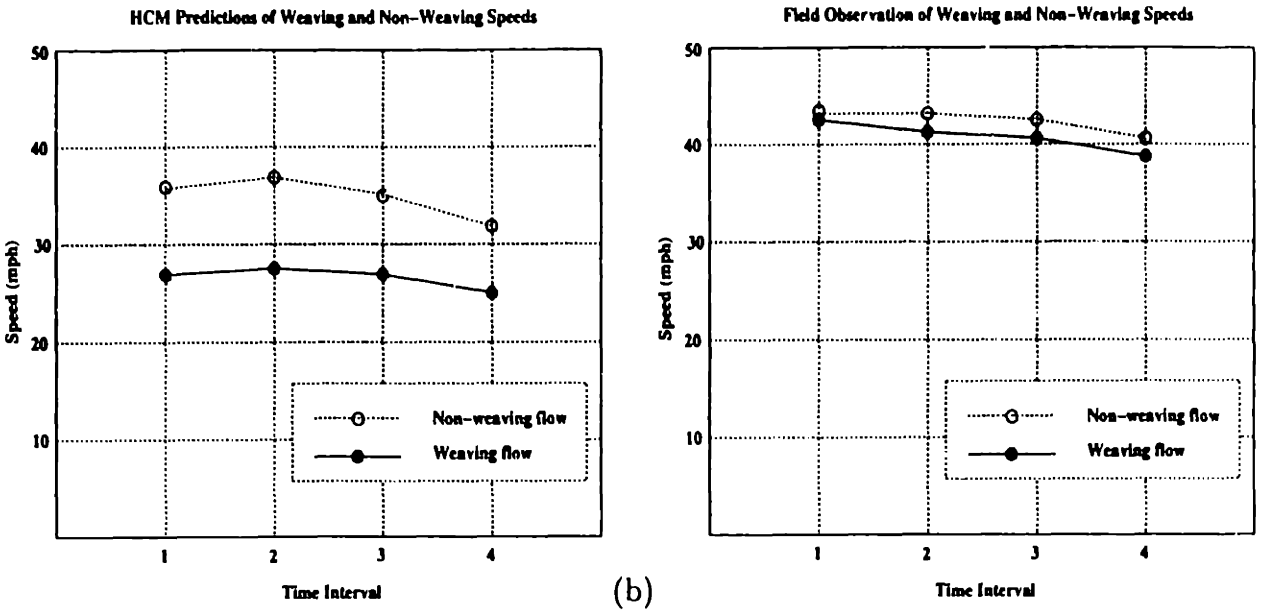

Figure 5.1: (a) HCM predictions of weaving and non-weaving speeds, and (b) Field observations of weaving and non-weaving speeds.

for weaving traffic, or 1.4 lanes. Therefore, the Capital Beltway network operates under constrained conditions according to the HCM prediction.

5.1.3 Calculation Results

To estimate the weaving and non-weaving speeds, we substitute the component flow information from Table 5.1, and the corresponding parameters for constrained operations, into the HCM weaving/non-weaving speed prediction formula, Equation 5.1. The prediction results for constrained operations are shown in Figure 5.1(a). For comparison, field observations of weaving and non-weaving speeds are shown in Figure 5.1(b).

Comparing the two figures, we find significant differences between the HCM predictions and the field observations.

1. The HCM method underestimates both weaving and non-weaving speeds for the

Capital Beltway network. HCM underestimates non-weaving speed by about $7 \sim 8$ mph, and weaving speed by $14 \sim 16$ mph.

2. According to the HCM calculations, a speed difference about $7 \sim 9$ mph is predicted to persist between weaving and non-weaving speeds. In other words, an unbalanced operation exists. In the field, very close weaving and non-weaving speeds are observed. The difference between weaving and non-weaving speeds is only about $1 \sim 2$ mph.

3. From the HCM calculations, we see that non-weaving speed increases slightly at first, to 37 mph, then drops continuously to the end, finishing at 32 mph. In the field, non-weaving speed was observed to be constant at 42 mph, then to drop by 2 mph when the traffic demand exceeded 1,800 veh/hr/lane.

4. From the HCM calculations, we see that weaving speed increases slightly at first, to 27 mph, then drops continuously to the end, finishing at 25 mph. In the field, weaving speed was observed to drop slightly to 41 mph at first, remain there for one 15-minute interval, and then to drop by 2 mph.

5.1.4 HCM Limit Checking

The HCM procedure described above can only be applied to certain situations. To check whether the calculation results are valid, we need to compare several measurements against the limits of HCM. The comparison is shown in Table 5.2.

The limitation check reveals that all key measurements are within set limits except

Table 5.2: HCM limit checking for Type A weaving area equations

parameters	HCM limits	calculation results
maximum v_w	1,800 pcph	mean 2,520 pcph stdev 32
maximum v/N	1,900 pcphpl	mean 1,725 pcphpl stdev 20
max VR (for 3 lanes)	0.50	0.34 - 0.36
max weaving length	2,000 ft	695 ft

for the weaving traffic volume v_w. The HCM limit for weaving flow is 1,800 pcph, thus the average weaving volume of 2,520 pcph on the Capital Beltway network clearly exceeds this range. This means that a breakdown is likely to happen in the network, and the predictions of weaving and non-weaving speeds may not be correct.

Table 5.3: Level of service (LOS) criteria for weaving sections (Source:[6])

LOS	min avg S_w (mph)	min avg. S_{nw} (mph)
A	55	60
B	50	54
C	45	48
D	40	42
E	35/30	35/30
F	< 35/30	< 35/30

The estimated values of S_w and S_{nw} are also used to assess the level of service (LOS) as recommended by the HCM in Table 5.3. Since non-weaving and weaving speeds are lower than the minimum weaving and non-weaving speed given for level of service F. The indication is that a breakdown may occur in the network, and that level-of-service

F may be present in the traffic.

5.2 Sensitivity Analysis

In this section, we will conduct two sensitivity analyses that examine HCM's and MIT-SIM's responses to changes in network geometry. Three new scenarios have been designed based on the original Capital Beltway network by changing the weaving length. The original network has a weaving length of 695 ft. The new scenarios have weaving lengths of 500 ft, 800 ft, and 1000 ft.

5.2.1 HCM Sensitivity Analysis

As we have seen in the previous section, the HCM predictions of weaving and non-weaving speeds for a type A weaving section are given by Equation 5.1. According to this equation, weaving and non-weaving speeds are functions of the weaving length. As weaving length increases, weaving and non-weaving speeds also increase. There are two operational explanations for this relationship:

1. Weaving length constrains the time and space in which the driver must make all required lane changes. As the length of a weaving area increases, the intensity of lane-change, and the resulting level of turbulence decrease, and hence, the level of service increases.

2. For a typical ramp-weaving section, the design speeds of ramps are usually lower than that of the freeway. Ramp vehicles must accelerate or decelerate as they traverse the weaving section. A longer weaving length provides more space for the

Table 5.4: HCM Weaving Length Sensitivity Analysis

Time Interval	Weaving Speeds				Non-Weaving Speeds			
	500 ft	695 ft	800 ft	1,000 ft	500 ft	695 ft	800 ft	1,000 ft
0 - 15 min	24.41	26.88	28.07	30.10	33.40	35.75	36.79	38.44
15 - 30 min	24.94	27.51	28.73	30.82	34.37	36.76	37.80	39.47
30 - 45 min	24.22	26.66	27.83	29.84	32.98	35.31	36.34	37.99
45 - 59 min	22.67	24.79	25.83	27.63	29.97	32.12	33.04	34.65

vehicles, making lane changes easier to execute, which results in higher level of service.

Using the procedure described in previous section, we have calculated for HCM's predictions of weaving and non-weaving speeds for the four scenarios of weaving lengths (500 ft, 695 ft, 800 ft, and 1000 ft). The results are shown in Table 5.4. From the table, we observe that:

- Weaving and non-weaving speeds increase as the weaving length increases. On average, an increase of 100 ft in the weaving length leads to an increase of $1.0 \sim 1.2$ mph in weaving and non-weaving speeds.

- In all the scenarios, constrained operations are predicted by the HCM method. A speed difference of $7 \sim 10$ mph is predicted to persist between weaving and non-weaving flows in every scenario.

- A weaving speed drop of $2.0 \sim 2.5$ mph is predicted between third and fourth time intervals when flow reaches the capacity of $1,800 \sim 2,000$ veh/hr/lane. The drop

Table 5.5: MITSIM Weaving Length Sensitivity Analysis

Time Interval	Weaving Speeds				Non-Weaving Speeds			
	500 ft	695 ft	800 ft	1,000 ft	500 ft	695 ft	800 ft	1,000 ft
0 - 15 min	42.03	42.65	42.38	45.00	42.28	43.80	42.93	44.78
15 - 30 min	41.23	41.43	42.88	45.05	42.73	42.97	44.05	44.53
30 - 45 min	39.45	40.37	43.27	42.00	42.23	38.68	44.97	38.65
45 - 59 min	35.65	35.95	38.40	39.02	33.10	33.90	37.98	36.93

seems to be independent of changes in weaving length. Similarly, a non-weaving speed drop of $3.5 \sim 4.0$ mph is also predicted.

5.2.2 MITSIM Sensitivity Analysis

The MITSIM sensitivity analysis is conducted using exactly the same inputs (except weaving length) as those used in the simulations of the Capital Beltway network, described in Chapter 4. We run MITSIM on the four scenarios which we have already tested with the HCM method. The weaving, non-weaving speeds, and average speeds of the four component flows are computed directly from MITSIM vehicle trajectory data. The simulation results are summarized in Table 5.5. The speeds of the four component flows over the twelve 5-minute intervals are shown in Figure 5.2. We observe that:

- In MITSIM, weaving and non-weaving speeds increase as the weaving length increases. On average, an increase of 100 ft in the weaving length results in an increase of $0.6 \sim 0.8$ mph in weaving and non-weaving speeds.

- Unlike HCM predictions, which are deterministic, MITSIM predictions are stochastic. The predicted weaving and non-weaving speeds in a longer weaving area are

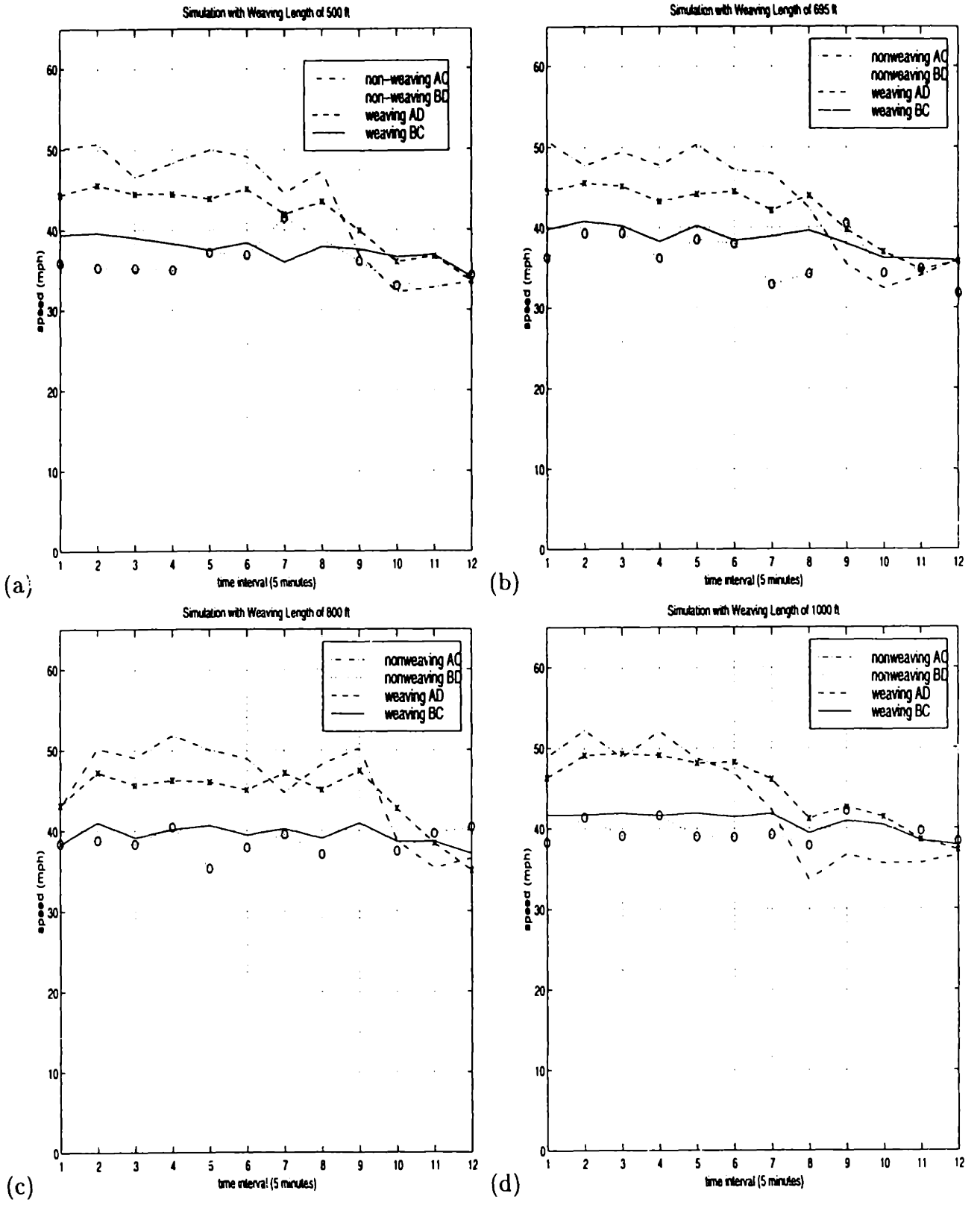

Figure 5.2: Weaving and non-weaving speed for various weaving lengths: (a) weaving length of 500 ft, (b) weaving length of 695 ft (Capital Beltway weaving length), (c) weaving length of 800 ft, and (d) weaving length of 1000 ft.

not necessarily always higher than those from a shorter weaving area.

- From Table 5.5, we observe very close weaving and non-weaving speeds until traffic flows approach capacity near the end. Therefore, MITSIM predicts unconstrained operations, while HCM predicts constrained operations.

- From Figure 5.2, it is observed that weaving speeds in the AD and BC directions change with the alterations of weaving length. As weaving length increases, the average speed in the AD direction increases steadily and gets close to 48 or 49 mph. When traffic flows reach capacity, consistent weaving speed drops are predicted for the AD direction in all the scenarios. As weaving length increases, the magnitude of the speed drops become smaller. Similar pattern of speed change is also observed for traffic flow in the BC direction.

- In all the cases, the speed in AC direction is about $48 \sim 50$ mph when traffic flow is lower than capacity, and drops to $34 \sim 36$ mph when traffic reaches capacity. The speed in BD direction is about $38 \sim 40$ mph for all time periods.

- Comparing the HCM predictions of weaving and non-weaving speeds with those of field observations, we find an under-estimation of $7 \sim 8$ mph for non-weaving speed and $14 \sim 16$ mph for weaving speed.

5.3 Summary

In this chapter, we tested the sensitivity of predicted weaving and non-weaving speeds to weaving length for MTISIM, and compare it to the sensitivity exhibited by the HCM. Four scenarios with weaving length of 500 ft, 695 ft, 800 ft, and 1,000 ft have been designed and tested. Our validation results show that the HCM method predicts constrained operations for all scenarios, while MITSIM predicts unconstrained operations.

Chapter 6

Conclusion and Future Research Direction

6.1 Summary and Conclusion

This research focuses on validating basic macroscopic traffic properties, the performance of MITSIM in simulating weaving traffic, and identifying calibration needs.

In Chapter 2, we briefly reviewed the MITSIM model structure and key parameters that control the component models, and presented main mathematical relationships between macroscopic traffic properties and microscopic model parameters.

In Chapter 3, we accessed the capacity predicted by MITSIM, and validated the basic macroscopic relationships on a simple 2-lane basic freeway section. We found that $2,000$ $veh/hr/lane$ can be accepted as the simulated capacity, which is identical to field observations documented in other work. Based on this finding, we then validated the flow-speed-density relationships using simulated sensor outputs. We found that: (i) the key parameters, which determine the operations of a freeway, were consistent with the field findings from the Santa Monica high-speed freeway (detector 16) in Los Angeles,

except for the optimum speed, which seems to be higher than those in the field; and (ii) the shapes of simulated flow-speed-density relationship were all similar to those found in the high-speed freeway data.

In Chapter 4, we further examined the ability of MITSIM in simulating these macroscopic properties under more complicated traffic conditions, and conducted a case study of a ramp-weaving section from the Capital Beltway network. On the macroscopic level, various simulated macroscopic measurements, namely, lane flow, speed, density, average speeds of component flows, and weaving and non-weaving speeds, were computed and compared with those from field, with emphasis on weaving and non-weaving speeds. On the microscopic level, simulated headway and lane change distributions were computed and compared with those from the field. Our results showed: (i) the capacity and flow-speed-density relationships predicted by MITSIM are very similar to those found in the field. (ii) MITSIM seems to simulate traffic flow, weaving and non-weaving speeds reasonably well; however, its performance in simulating lane speed and density needs improvement; (iii) the simulated headways have different patterns from those of the field, and the simulated mandatory lane changes are too intensive around the on-ramp junction, while the discretionary lane changes are too intensive in the weaving area.

They indicate that: (i) weaving activities predicted by MITSIM are too concentrated. (ii) h_{upper} may be too high. (iii) more calibrations and testings of the lane-change model are needed.

Finally, we evaluated the sensitivity of MITSIM to the weaving length. We computed and compared the simulation results of weaving and non-weaving speeds with those from the HCM. Our validation results showed that MITSIM is sensitive the weaving length, and can give reasonable predictions. The sensitivity is compared to the sensitivity of HCM. By adding the systematic biases of HCM, we found that the HCM predictions are very similar to those from MITSIM. We concluded that MITSIM gives better performance than HCM in predicting weaving and non-weaving speeds.

6.2 Thesis Contributions

The main contributions of this thesis are:

1. assessed the capacity predicted by MITSIM (Ch 3).

2. validated basic macroscopic traffic relationships using sensor outputs from MITSIM (Ch 3).

3. studied the ability of MITSIM to replicate the traffic characteristics of a weaving section using field trajectory data (Ch 4).

4. compared HCM predictions of weaving and non-weaving speeds with those from MITSIM simulations (Ch 5).

5. conducted a sensitivity analysis of weaving length and compared the sensitivities of MITSIM predictions with those of HCM (Ch 5).

6.3 Future Research Directions

Further work in the area can be pursued along the following directions:

- Validation and calibration using other important freeway facilities. In this thesis, we have presented a case study of a ramp-weaving section. The validity of MITSIM for other freeway sections, such as ramp and ramp junctions, Type B and Type C weaving sections, is still pending.

- Incident analysis. A very important application of MITSIM is in capacity analysis, where traffic congestion and capacity reduction are the main concerns. In the thesis, we only examined a case of recurrent traffic congestion.

- Signalized Intersection. Calibrations and validations of MITSIM using typical urban network with signalized intersection is another important activity.

- Calibration of lane-changing and car-following models. In this research, we have computed very useful distributions of lane-changes and time headways. Unfortunately, due to thesis limitation, we do not have enough time to fit the distribution curves and incorporate them into the MITSIM models.

Bibliography

[1] Q. Yang and K. N. Koutsopoulos. A microscopic traffic simulator for evaluation of dynamic traffic management systems. *Transportation Research C*, 4(3):113–129, 1996.

[2] H. Subramanian. Estimation of a car-following model for freeway simulation. Master's thesis, Massachusetts Inst. of Tech., Cambridge, MA, 1996.

[3] Ahmed, Ben-Akiva, Koutsopoulos, and Mishalan. Models for freeway lane changing and gap acceptance behavior, *Proceedings of 13th International Symposium on Transportation and Traffic Theory*, Lyon France, 1996.

[4] Kazi I. Ahmed, Modeling Freeway Lane Changing Behavior. Master's thesis. Massachussets Instidute of Technology, 1996.

[5] Qi Yang. A simulation Laboratory for Evaluation of Dynamic Traffic Management Systems. Doctoral Dissertation, Massachussets Institute of Technology, 1997.

[6] *Highway Capacity Mannual*, 1994. Special Report 209, *Third Edition*, Transportation Research Board, National Research Council, Washington D.C., 1994.

[7] Michael J. Cassidy, Jun Han, Validation and Evaluation of Freeway Simulation Models. Final Technical Report, FHWA. Purdue-RR-95-1.

[8] H. N. Koutsopoulos and Q. Yang. Modeling requirements for emerging transportation system operating environments. Report DTRS-57-88-C-0078, TTD 29, John A. Volpe National Transportation Systems Center, Cambridge, MA, 1992.

[9] FHWA. Development and testing of INTRAS: a microscopic freeway simulation model - Vol. 1-3. Report FHWA/RD-80/106-108, Federal Highway Administration, US-DOT, McLean, Virginia, 1980.

[10] FHWA. FRESIM User Guide. Technical Report Version 4.5, Federal Highway Administration, US-DOT, McLean, Virginia, 1994.

[11] S. W. Sibley. NETSIM for microcomputers - simulates microscopic traffic flow on urban streets. *Public Roads*, 49, 1985.

[12] FHWA. CORSIM User Guide. Technical Report Version 1.0, Federal Highway Administration, US-DOT, McLean, Virginia, 1996.

[13] D. K. Codelli, W. P. Niedringhaus, and P. Wang. The Traffic and Highway Objects for REsearch, Analysis, and Understanding THOREAU IVHS model, Vol.I. Technical Report MTR 92W208V1, MITRE, McLean, Virginia, 1992.

[14] F. Middelham, T. Wang, R. Koeijvoets, and H. Taale. FLEXSYT-II: Manual - Vol. 1-2. Technical report, Transport Research Center (AVV), Ministry of Transport, Public Works and Water Management, the Netherlands, 1994.

[15] J. Barcelo and J. L. Ferrer. A simulation study for an area of Dublin using the AIMSN2 traffic simulator.

[16] H. J. Payne. FREFLO: A macroscopic simulation model of freeway traffic: Version 1 - User's guide. Technical report, ESSOR Report, 1978.

[17] Y. Sheffi, H. Mahmassani, and W. B. Powell. A transportation network evaluation model. *Transportation Research*, Vol 16A(3), 1982.

[18] J. F. Gilmore, S. P. Roth, H. C. Forbes, and K. A. Payne. ATMS universal traffic operation simulation. 5th IVHS America Annual Meeting, Washington, D.C., 1995.

[19] A. Messmer and M. Papageorgiou. METANET: A macroscopic simulation progrm for motorway networks. *Traffic Engineering & Control*, 31(8/9):466-477, 1990.

[20] H. Haj-Salem, N. Elloumi, S. Mammar, M. P. J. Chrisoulakis, and F. Middelham. METACOR: A macroscopic modelling tool for urban corridor.

[21] A. de Palma, F. Marchal, and Y. Nesterov. METROPOLIS: A modular system for dynamic traffic simulation. http://www.ceic.com/metro/, 1996.

[22] M. van Aerde and S. Yagar. Dynamic integrated freeway/traffic signal networks: A routing-based modeling approach. *Transportation Research A*, Vol. 22A(6):445-453, 1988.

[23] M. van Aerde. INTEGRATION: A dynamic traffic simulation/assignment model. Paper presented at the IVHS Dynamic Traffic Assignment and Simulation Workshop, Federal Highway Administration, 1992.

[24] Ruey L. Cheu, Wifred W. Recker, Stephen G. Ritchie. Caliberation of INTRAS for Simulation of 30-Second Loop Detector Output. Transportation Research Board,72th Annual Meeting, Jan. 10-14, 1993. Washington D.C.

[25] R.F.Benekohal. Development and Validation of a Car Following Model for Simulation of Traffic Flow and Traffic Weav Studies at Bottlenecks. Ph.D. dissertation, Ohio State University, Columbus, 1986.

[26] S. A. Smith. Freeway data collection for studying vehicle interactions. Technical Report FHWA/RD-85/108, Federal Highway Administration, Office of Research, Washington D. C., 1985.

[27] Adolf D. May. Traffic Flow Fundamentals. Printice Hall,1990.

[28] J. S. Drake, J. L. Schofer and A. D. May, A Statistical Analysis of Speed Density Hypotheses, *in Third International Symposium on the theory of Traffic Flow Procedings*, Elsevier North Holland, Inc., New York, 1967.

[29] Avishai Cedar and Adolf D. May, Futher Evaluation of Single abd Two-Regime Traffic Flow Models, Transportation Research Board, Record 567, TRB, Washington D. C., 1976, pages 1-15.

[30] A. D. May, Jr. and H. E. Keller, Non-integer Car-Following models, Highway Research Board, Record 199, HRB, Washington D. C., 1967, pages 19-32.

[31] R.S. Sargent, Verification and Validation of Simulation Models: *Progress in Modeling and Simulation*, F.E. Cellier (ed.), Academic Press, New York, 1982

[32] R.F.Benekohal, Procedure for Validation of Microscopic Traffic Flow Simulation Models, *Transportation Research Record 1320*, pp.190-202, 1993.

[33] Robert S. Pindyck and Daniel L. Rubinfeld,Econometric models and economic forecasts, McGraw-Hill, Inc.(3rd), 1991.

[34] Hideyuki Kita, Effects of Merging Lane Length on the Merging Behavior at Expressway On-Ramp, *Transportation and Traffic Theory/C.F. Daganzo (Editor)*, pp.37-51,1993.

[35] Michaels, R.M. and J. Fazio, Driver Behavior Model of Merging, TRR, No.1231,pp.4-10,1989.

[36] Makigami.Y and T. Matsuo, A Merging Probability Calculation Method Considering Multiple Merging Phenomena, Proc. of the 11th Int. Symp. on Transportation and Traffic Theory, Elsevier Science Pub. Co., pp.21-38, 1990.

[37] Cassidy, M., A proposed Analytical Technique for the Design and Analysis of Major Freeway Weaving Sections, Ph.D. Dissertation, University of California at Berkeley, 1990.

[38] D.C. Gazi, R. Herman, and R. Potts, Car-flowing Theory of Steady-State Traffic Flow, Operations Research, Vol.7, 1959, pages 499-595.

[39] A.D.May, Jr. and H.E.M.Keller, Non-integer Car-following Models, Highway Research Board, Record 199, HRB, Washington D. C., 1967, pages 19-32.

[40] A.D.May, Jr. and H.E.M.Keller, Evaluation of Single and Two-Regime Traffic Flow Models. Fourth International Symposium on the Theory of Traffic Flow Proceedings, Karlsruhe, West Germany, 1968.

[41] L. A. Pipes, An Operational Analysis of Traffic Dynamics, Journal of Applied Physics, Vol. 24, No.3, 1953, pages 274-287.

[42] D. C. Gazis, R. Herman, and R. W. Rothery, Non-linear Follow-the-Leader Models of Traffic FLow, Operations Research, Vol.9, No.4, 1961, pages 545-567.

[43] B. D. Greenshields, A study un Highway Capacity, Highway Research Board, Procedings, Vol. 14, 1935, page458.

[44] H. Greenburg, An Analysis of Traffic Flow, Operations Research, Vol.7, 1959, pages 78-85.

[45] R. T. Underwood, Speed, Volume and Density Relationships. Quality and Theory of Traffic Flow, Yale Bureau of Highway Traffic, New Haven,Conn., 1961, pages 141-188.

[46] L. C. Edie, Following the Steady State Theory for Non-congested Traffic, Operations Research, Vol. 9, 1961, pages 66-76.

[47] D. R. Drew, Deterministic Aspects of Freeway Operations and Control. Texas Transportation Institute, Research Report 24-4, June 1965.

[48] Nakamura, H., M.Kuwahara and M. Koshi, A Simulation Model for the Evaluation of Weaving Capacity, *Highway Capacity and Level of Service (Brannolte, U.(ed.)*, pp.259-270, Balkema, Rotterdam, 1991.

[49] J.F.Torres, A. Halati and A. Gafarian *Statistal Guidelines for Simulation Experiments.* Exexutive Summary, JFT Associates, Culver City, 1983.

[50] A.V.Gafarian and J.D Walsh. Methods for Statistical Validation of a Simulation Model for Freeway Traffic Near an On-Ramp, *Transportation Research*, Vol.4, 1970, pp.324-379

[51] J.P.C.Kleijnen. *Design and Analysis of Simulations: Practical Statistical Techniques*, SCI Simulation, Vol.28, No.3, March 1977.

[52] J.P.C.Kleijnen. Computing Means and Variances of Two Simulations. SCI Simulation, Vol.26, No.3, March 1976.

[53] G.S.Fishman, Problems in the Statistical Analysis of Simulation Experiments: The Comparison of Means and the Length of Sample Records, Communications of the ACM. Vol.10, No.2, 1967, pp.94-99.

[54] D. Wicks et al, Development and Testing of INTRANS, a Microscopic Freeway Simulation Model, Volume 3, Validation and Application, Final Report, FHWA/RD-80/108. FJWA, U.S. Department of Transportation, 1980.

[55] Panos Michelopoulos, Eil Kwon, and Jeong-Gyu Kang, Enhancement and Field Testing of a Dynamic Freeway Simulation Program, *Transportation Research Record 1320*, pp203-215, 1993.

[56] Yasuji Makigami and Takao Iizuka, Evaluation of Weaving Traffic Stream Using Merging Probability, *Transporation and Traffic Theory/C.F. Daganzo(Editor)*, 1993.

[57] Joshi, S. S.; Rathi, A. K.; Statistical Analysis and Validation for Multipopulation Traffic Simulation Networks, *Transportation research record*, 1510, pp. 35-44, 1995.

[58] Gallimore, Shane C., "Validation of the Mesoscopic Event-driven Traffic Simulation Model", Thesis (B.S.)–California Polytechnic State University, 1995.

[59] Horiguchi, R.; Kuwahara, M.; Nishikawa, I., The Model Validation of Traffic Simulation System for Urban Road Networks: AVENUE. Intelligent transport systems

Proceedings of the 2nd world congress on intelligent transport systems, Nov. 1995, Yokohama,Japan.

[60] Tudge, R. T., INSECT, the calibration and validation of an intersection simulation model, *Intersections without traffic signals.*,Berlin ; New York :,Springer-Verlag, c1988.

[61] Helbing, D, Derivation and empirical validation of a refined traffic flow model, Physica A, Volume 233, Number 1-2, pp. 253,1996.

[62] Yukawa, Satoshi; Kikuchi, Macoto, Density Fluctuations in Traffic Flow, *Journal of the Physical Society of Japan*, Volume 65, Number 4, pp. 916, 1996.

[63] Rakha, H; Aerde, M Van, 'Statistical Analysis of Day-to-Day Variations in Real-Time Traffic Flow Data, *Transportation research record*, No. 1510, pp. 26,1995.

[64] Nakatsuji, Takashi; Tanaka, Mitsuru; Nasser, Pourmoallem;Hagiwara, Toru, Description of Macroscopic Relationships Among Traffic Flow Variables Using Neural Network Models, *Transportation research record*, No. 1510,pp. 11,1995.

[65] Pursula, Matti, DISCUSSION- Another Look at A Priori Relationships Among Traffic Flow Characteristics, *Transportation research record*, No. 1510, pp. 10,1995.

[66] Cassidy, Michael, DISCUSSION - Another Look at A Priori Relationships Among Traffic Flow Characteristics, *Transportation research record*, No.1510,pp. 9,1995.

[67] Banks, James H, Another Look at A Priori Relationships Among Traffic Flow Characteristics, *Transportation research record*, No.1510,pp. 1,1995.

[68] Whittingham, A., Investigation of traffic speed, flow and geometry in urban areas, Transportation planning methods : proceedings of Seminar C held at the PTRC Transport and Planning Summer Annual Meeting, University of Sussex, England, from 11-15 September 1989.

[69] Jain, S. S.; Gupta, A. K.; Tiwari, Davesh, A Conceptual Approach for Capacity Analysis and Level-of-Service for at-Grade Unsignalised Intersections Under Mixed Traffic Flow, *Highway research bulletin*, No.45, 1991.

[70] Iwasaki, Masato, Empirical Analysis of Congested Traffic Flow Characteristics and Free Speed Affected by Geometric Factors on an Intercity Expressway, *Transportation research record*, No. 1320, 1991.